Life Sciences 309 (2022) 121044

Contents lists available at ScienceDirect

Life Sciences

journal homepage: www.elsevier.com/locate/lifescie

# GC–MS analysis, and evaluation of protective effect of *Piper chaba* stem bark against paracetamol-induced liver damage in Sprague-Dawley rats: Possible defensive mechanism by targeting CYP2E1 enzyme through in silico study

Chandan Sarkar [a], Milon Mondal [a], Khattab Al-Khafaji [b], Dina M. El-Kersh [c], Sarmin Jamaddar [a], Pranta Ray [a], Uttam Kumar Roy [a], Mirola Afroze [d], Md. Moniruzzaman [d], Mala Khan [d], Umma Hafsa Asha [a], Abul Bashar Ripon Khalipha [a], Edna Mori [e], Bruna Caroline Gonçalves Vasconcelos de Lacerda [e], Isaac Moura Araújo [f], Henrique Douglas Melo Coutinho [f,*], Manik Chandra Shill [g], Muhammad Torequl Islam [a,*]

[a] Department of Pharmacy, Bangabandhu Sheikh Mujibur Rahman Science and Technology University, Gopalganj 8100, Bangladesh
[b] College of Dentistry, The University of Mashreq, Baghdad, Iraq
[c] Pharmacognosy Department, Faculty of Pharmacy, The British University in Egypt (BUE), El Shorouk, Cairo Governorate, Egypt
[d] Bangladesh Reference Institute for Chemical Measurements (BRiCM), Dr. Qudrat- e- Khuda Road (Laboratory Road), Dhanmondi, Dhaka 1205, Bangladesh
[e] CECAPE - College of Dentistry, Av. Padre Cícero, 3917 - São José, Juazeiro do Norte, CE 63024-015, Brazil
[f] Department of Biological Chemistry, Regional University of Cariri (URCA), Crato, Ceará 63105-000, Brazil
[g] Department of Pharmaceutical Sciences, North South University, Bashundhara, Dhaka 1229, Bangladesh

ARTICLE INFO

*Keywords:*
GC–MS
Piper chaba
CYP2E1

ABSTRACT

The present study attempted to scrutinize the protective effect of the methanolic extract of *P. chaba* stem bark against paracetamol-induced hepatotoxicity in Sprague−Dawley rats, along with the gas chromatography–mass spectrometry (GC–MS) analysis to identify phytochemicals, which were further docked in the catalytic site of CYP2E1 and the MD simulation for system that plays a major role in the bio-activation of toxic substances that produce reactive metabolites, leading to hepatotoxicity. *P. chaba* stem methanol extract (250 and 500 mg/kg) were treated orally with the negative control and the negative control silymarin (50 mg/kg) groups. Phytochemical profiling was conducted using GC–MS. In in-silico studies, PyRx software was used for docking analysis and the stability of the binding mode in the target active sites was evaluated through a set of standard MD-simulation protocols using the Charmm 27 force field and Swiss PARAM. Co-administration of *P. chaba* at both doses with APAP significantly reduced the APAP-augmented liver marker enzymes ALT, AST, ALP, and LDH, along with serum albumin, globulin, hepatic enzymes, histopathological architecture, lipid profiles, total protein, and total bilirubin, and elevated the levels of MDA. The GC–MS analysis indicated that *P. chaba* extract is enriched in fatty acid methyl esters (46.23 %) and alkaloids (10.91 %) and piperine is represented as a main phytochemical. Among all the identified phytochemicals, piperine (−8.0 kcal/mol) was found to be more interacting and stable with the binding site of CYP2E1. Therefore, all of our findings may conclude that the *P. chaba* stem extract and its main compound, piperine, are able to neutralize APAP-induced hepatic damage.

## 1. Introduction

Human liver disease, which is a global concern, is one of the most serious illnesses, causing a considerable share of morbidity and mortality in people of all ages [1]. According to the World Health Organization (WHO), there are roughly 170 million chronic hepatitis C patients worldwide, with 3–4 million people added to the list each year [2]. In addition, more than two million individuals die each year from liver diseases throughout the world [3].

The liver is an important organ in energy metabolism and xenobiotic

* Corresponding authors.
*E-mail addresses:* hdmcoutinho@gmail.com, hdmcoutiinho@urca.br (H.D.M. Coutinho), dmt.islam@bsmrstu.edu.bd (M.T. Islam).

https://doi.org/10.1016/j.lfs.2022.121044
Received 15 August 2022; Received in revised form 30 September 2022; Accepted 2 October 2022
Available online 5 October 2022

biotransformation [4]. Therefore, chronic exposure to harmful xenobiotics is likely to result in liver damage, which can induce cirrhosis, liver cancer, and abrupt liver failure [5,6]. Acetaminophen (also known as *N*-acetyl-para-aminophenol (APAP) or paracetamol) is a commonly used analgesic and antipyretic medication [7]. APAP is regarded safe at therapeutic levels (up to 4000 mg/day), but at greater concentrations, it can cause centrilobular necrosis, which is usually fatal [8]. More than 90 % of APAP is metabolized in the liver to non-toxic sulfate and glucuronide, with the remainder being transformed to a hazardous metabolite termed *N*-acetyl-p-benzoquinone imine (NAPQI) by cytochrome P450 (CYP) under normal circumstances (Fig. 1) [9]. Through a reaction with glutathione peroxidase, NAPQI, a hepatotoxic reactive molecule, is detoxified to diverse non-reactive compounds [5]. When NAPQI is produced in excess while taking additional acetaminophen, the depletion of glutathione (GSH) concentration results in hepatotoxicity [10]. However, when glutathione levels are low, NAPQI increases the generation of reactive oxygen species (ROS) such as superoxide, hydrogen peroxide, and hydroxyl radicals. As a result, an imbalance in the creation and elimination of free radicals caused oxidative stress [11]. As a result of the oxidative stress, mitochondrial peroxynitrite is formed, which causes mitochondrial DNA damage, and activated hepatic macrophages produce pro-inflammatory cytokines such as tumour necrosis factor alpha (TNF-α), interleukin- 6 (IL)-6, and IL-1, further progressing APAP-induced liver injury [12].

In the liver, APAP is detoxified in phases I and II; phase II conjugation enzymes, such as UDP-glucuronosyltransferases (UGTs) and sulfotransferases, recover the majority of APAP as APAP-gluc and APAP-sulf (SULTs) (Fig. 2) [13]. Induction of antitoxic phase II enzymes may hasten the metabolic inactivation of APAP, resulting in a decrease in APAP metabolized by CYP2E1 to NAPQI and relief from APAP liver toxicity [14]. Unfortunately, the present treatment options for liver illnesses are primarily ineffective, typically have major side effects, and are prohibitively expensive, particularly in underdeveloped countries [15]. The treatment agent's main characteristics are its great efficacy and minimal risk of adverse effects. Thus, the development of new and more potent hepatoprotective medicines with fewer side effects is required. Under these conditions, constant attempts have been made to find and develop a natural product-based efficient and safe CYP2E1 inhibitor that can regulate greater CYP2E1 activity while also reducing the harmful effects of hazardous metabolites produced.

Nature is regarded as the finest source of medicine for the abundance of natural compounds with potential therapeutic benefits [16]. As more and more conventional synthetic medications fail, there is growing acknowledgment of medicinal plants as potential sources for novel therapeutic compounds that are effective not only for hepatotoxicity but also for cancer, neurological disorders, and etc. [17,18]. For instance, we can see that the role of cruciferous vegetables and their vital bioactive compounds along with flavonoids in the treatment and prevention of colon cancer [19,20]; *Lepidagathis hyaline* [21], *Andrographis paniculata* [22], and *Alstonia scholaris* [23] could be a potential source of different pharmacological agents such as antidepressant, anti-oxidative, anxiolytic, cytotoxic, thrombolytic, and antimicrobial; *Ophiorrhiza rugosa* and *Spirulina platensis* have shown central and peripheral pain intervention as well as anti-inflammatory activity [24,25]; and Terpineol, a monoterpenoid alcohol, has shown immunomodulatory and neuroprotective effects [26].

*Piper chaba* Hunter, belonging to the family Piperaceae, is a glabrous climbing shrub popularly known as 'Chui Jhal' or 'Choi Jhal', which is

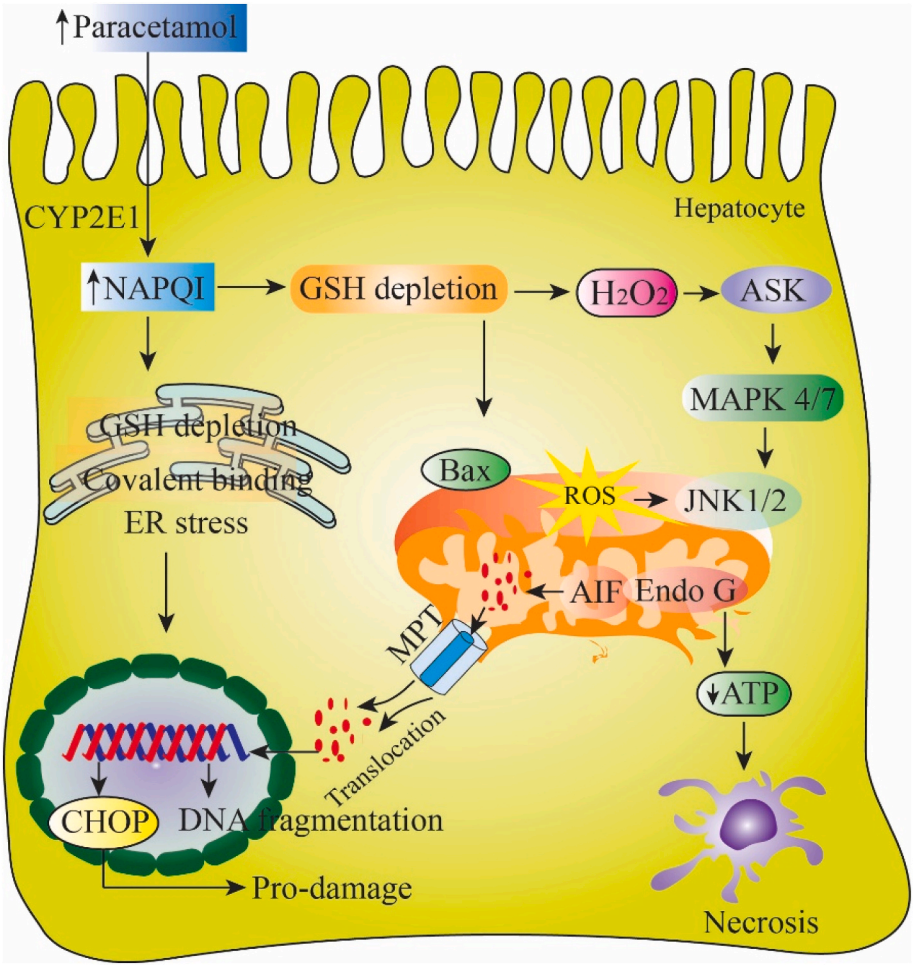


**Fig. 1.** Possible mechanism of APAP-induced hepatotoxicity. Overdosing on APAP causes the production of NAPQI, which depletes GSH in the mitochondria, ER, and cytoplasm and causes oxidative stress in these organelles, resulting in ATP reduction and the opening of the MPT pore, as well as the translocation of mitochondrial proteins (AIF and Endo G) to the nucleus. This causes nuclear DNA breakdown, which leads to necrotic cell death. [ASK1, Apoptosis signal-regulating kinase 1; AIF, apoptosis inducing factor; BAX, Bcl-2-associated X protein; CHOP, C/EBP Homologous Protein; ER, endoplasmic reticulum; GSH, glutathione; JNK, c-Jun N-terminal kinase; MKK4/7, mitogen-activated protein kinase 4/7; MPT, mitochondria permeability transition; NAPQI, *N*-acetyl-p-benzoquinone imine; ROS, reactive oxygen species].

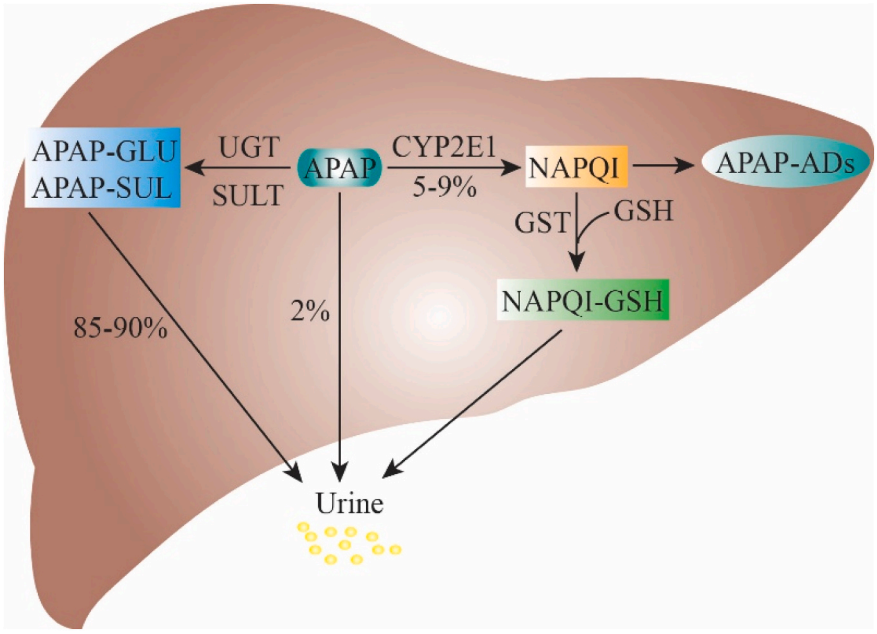


**Fig. 2.** Acetaminophen metabolic activation. Phase II conjugating enzymes (mainly UGT and SULT) are responsible for 85–90 % of APAP metabolism. Only 2 % of it is eliminated in the urine undamaged. And CYP 2E1 is responsible for around 5–9 % of the total, which is converted into the highly reactive intermediate metabolite NAPQI. NAPQI is often detoxified by conjugating with GSH. Following an APAP overdose, however, high NAPQI depletes GSH, resulting in the creation of APAPADs due to covalent sulfhydryl group attachment in cellular proteins. [APAP, acetaminophen; APAP-ADs, APAP protein adducts; CYP 2E1, Cytochrome P450 2E1; GSH, glutathione; NAPQI, *N*-acetyl-p-benzoquinone imine; SULT, sulfotransferase; UGT, UDP-glucuronosyltransferase].

most commonly used in Bangladesh and India as a spice and also conceived to have ethnobotanical properties for a wide range of diseases, including bronchitis, asthma, piles, arthritis, colic pain, dyspepsia, and gastralgia [27,28]. Moreover, the aerial section of this plant exhibits analgesic, carminative, diuretic, expectorant, stimulant, and smooth muscle relaxant properties [29,30]. The fruits, on the other hand, have anti-tussive, anti-flatulent, erythropoietic, expectorant, and palatable characteristics [31,32], whereas the stem is used to treat diarrhea and rheumatic pains, as well as to relieve post-partum discomfort in mothers [33]. Traditionally, in different countries, it is used as a gastro-protective, anti-flatulent, appetizing property, as an antitussive, expectorant, and anti-fungal agent. It can also be used to decrease cholesterol and as part of a digestive and sleep-inducing preparation [34].

In a literature review, Islam and his colleagues reported that *P. chaba* exhibits different biological activities including anti-inflammatory, analgesic, anti-diarrheal, anti-diabetic, anti-microbial, anti-parasitic, anti-malarial, anti-leishmanial, adipogenic, cytotoxic/anticancer, gastro-protective, anti-ulcer, diuretic, depressive, anti-hypertensive, antipyretic, and immunomodulatory effect [35]. On the other hand, Matsuda et al. (2009) demonstrated that the aqueous acetone extract from the fruit of *P. chaba* exhibits hepatoprotective effects against lipopolysaccharide (LPS)-induced liver injury in mice [36].

Although the hepatoprotective effect of the fruit of *P. chaba* has been reported, the hepatoprotective effect of the stem bark of *P. chaba* against APAP-induced liver toxicity and its underlying mechanisms by targeting CYP2E1 and especially how the plant active compounds interact with this target to afford liver protection are not yet clear. Therefore, the objective of this experiment was to evaluate the protective effect of methanolic extract of the stem bark of *P. chaba* on APAP-induced liver damage in rats. Thus, the current study was undertaken to determine: (i) the phytochemical profile of the methanolic extract of stem bark by gas chromatography–mass spectrometry (GC–MS); (ii) the hepatoprotective effect of this extract through an antioxidative defense mechanism against APAP-induced liver damage in Sprague-Dawley rats; and (iii) how strongly, actively, stably, and specifically the active compounds identified from this extract bind to the target CYP2E1 with the help of in silico docking study and molecular dynamics protocols.

## 2. Materials and methods

### 2.1. Chemicals and reagents

#### 2.1.1. Sample collection and extract preparation

In January 2020, stem portions of *P. chaba* were obtained from local markets in Khulna and Bagerhat, Bangladesh. It was identified by a taxonomist from the Bangladesh National Herbarium (BNH) Mirpur, Dhaka, Bangladesh. A voucher specimen, number 43198, was deposited there. To make it suitable for grinding, stem sections were cleansed with tap water, sun-dried, and then dried again at a moderate (40 °C) temperature. The dried components were ground into fine powder using a blender (CM/L7360065, Jaipan and Mumbai, India). A Soxhlet apparatus (Z556203, Aldrich® Soxhlet extraction equipment, Darmstadt, Germany) was used to extract 1200 g of sample powder at 65 °C using methanol (6000 mL) as a solvent to create a 20 % methanolic extract [37]. The extract was then filtered using Whatman 1 filter paper and dried using rotary evaporation at 40 ± 2 °C under reduced pressure (100 psi). The yield was 321.94 g, and the gummy concentration was collected and kept at 20 °C for future investigation and pharmacological property evaluation.

#### 2.1.2. Phytochemicals identification through GC–MS analysis

Gas Chromatography-Mass Spectroscopy (GC–MS with triple quadropole, GC: Agilent 7890A, USA and MS: Agilent 5975C, USA) on a capillary column (5 % Phenyl Methyl Siloxane; DB-5MS (30 m × 0.250 mm × 0.25 m) was used to examine the phytochemicals in *P. chaba* stem methanol extract [38]. Initially, 1.0 μL liters of material were injected into the GC column's injection port in splitless mode at a constant flow rate of 1 mL per minute. The injection temperature was preserved at 230 °C, and the procedure was carried out with helium gas (99.99 % pure). Using a temperature control system, the initial column oven temperature was set at 60 °C for 1 min, then 10 °C/min to 200 °C for 2 min, and lastly 12 °C/min to 300 °C for 5 min, for a total run duration of 30 min. For the GC–MS studies, the following detector settings were used: 250 °C interface temperature, 230 °C ion source temperature, and mass spectrometry with scan, $m/z$ 50–600 scanning range, scan speed mode 2000, and a scan duration of 0.3 s for each scan. The peak area represents the extracted constituents' relative percentage. The compounds were identified by matching the spectrum configurations

obtained with those in the accessible mass spectral National Institute of Standards and Technology (NIST) collection.

### 2.2. Assessment of hepatoprotective effect

#### 2.2.1. Animals

The rats utilized in this study were locally bred adult healthy male Sprague-Dawley rats (140–180 g) obtained from the Department of Pharmacy, Jahangirnagar University (Bangladesh). For one week prior to the studies, these animals were maintained at the Animal House of the Department of Pharmacy, Jahangirnagar University, Bangladesh, under conventional laboratory settings of constant temperature (25 ± 2 °C), humidity (55 5 %), and 12 h light/dark cycles [39]. Animals were allowed unrestricted access to a standard meal and water, and they were housed according to the Animal By-Laws established by Jahangirnagar University's Biosafety, Biosecurity, and Ethical Committee [approval number: BBEC, JU/M 2018 (1)3].

#### 2.2.2. Acute toxicity study

According to the OECD standard, 30 Sprague-Dawley rats were randomly split into five groups, each with six animals [40]. Different doses of methanol extract (250, 500, 1000, 2000, and 4000 mg/kg body weight) were given orally and delivered into the stomach through the esophagus with the use of a stainless-steel needle linked to a plastic syringe. The animals were then examined for evidence of toxicity and death (i.e., weight loss, general behavior, respiratory pattern, cardiovascular signs, motor activities, reflexes, and changes in skin and fur texture) [41].

### 2.3. Experimental design

The study used a paracetamol-induced hepatotoxicity model, according to Rajasekaran and Periyasamy [42]. The rats were divided into five groups, each consisting of seven Sprague-Dawley rats (*Rattus norvegicus*). For 14 days, the normal control received 2 mL/rat body weight of normal saline. The negative control was given 2 mL/rat of normal saline, while the treatment I and treatment II groups were given 250 and 500 mg/kg of *P. chaba* stem methanol extract, respectively. Both doses were chosen based on the results of an acute toxicity investigation. The standard group got 50 mg/kg BW of silymarin (p.o.). All rats except those in the normal control group were administered paracetamol orally on the 15th day at a dose of 2 g/kg body weight. The animals were sacrificed 24 h after receiving paracetamol, and blood samples and liver tissues were obtained for biochemical and histological analysis, as shown below [43]. Centrifugation (3000 rpm for 10 min) was used to separate blood serum, which was then kept at −20 °C. Each rat's liver was dissected and cleaned in ice cold saline to remove blood and debris before being kept at −40 °C until further investigation. Following that, liver samples were homogenized in phosphate buffer saline (25 mM, pH 7.4) to form a homogenate that was roughly 10 % (w/v). The supernatant was collected and utilized to evaluate liver enzymatic and non-enzymatic reduced antioxidants, as well as Thiobarbituric acid reactive substances (TBARS) levels, after centrifugation at 4000 rpm and 4 °C for 15 min [44].

#### 2.3.1. Evaluation of biochemical parameters in serum

We determined the biochemical parameters for liver function including serum alanine aminotransferase (ALT), aspartate aminotransferase (AST), alkaline phosphatase (ALP), γ-glutamyl-transferase (GGT) and lactate dehydrogenase (LDH), total bilirubin (TB), total protein (TP), albumin (ALB), globulin (GLB), triglycerides (TG), total cholesterol (TC), high density lipoprotein cholesterol (HDL—C) and low density lipoprotein cholesterol (LDL-C) levels by following the standard protocols of human commercial kits and by using Humalyzer 3500 (Human, Wiesbaden, Germany) [45].

#### 2.3.2. Lipid peroxidation assay

A conventional experimental approach was used to assess thiobarbituric acid reactive substances (TBARS), a prominent biomarker of lipid peroxidation (LPO) [46]. In a nutshell, 0.2 mL of liver homogenate tissue was combined with 0.2 mL sodium dodecyl sulfate (8.1 %), 1.5 mL acetic acid (20 %), and 1.5 mL thiobarbituric acid (8 %). 4 mL of distilled water was then added, and the mixture was cooked in a water bath for 60 min at 95 °C. 5 mL of a butanol:pyridine (15:1) combination was added once the liquid had cooled to room temperature. The contents of the combination were vortexed for 2 min before being centrifuged at 3000 rpm for 10 min and the upper organic layer collected. The level of lipid peroxidation was represented as nmol of thiobarbituric acid reactive substances (TBARS) per mg of protein, and the absorbance was measured at 532 nm against a blank [47].

#### 2.3.3. Evaluation of reduced glutathione (GSH) levels

With minor modifications, reduced GSH was found using Islam's approach [48]. For the first 5 min, 1 mL of liver homogenate was combined with the same quantity of 10 % TCA and incubated. The mixture was then separated by centrifugation at 2000 rpm for 10 min at 4 °C. The supernatant was then combined with 5 mL of 0.2 M PBS (pH 8) and 2 mL of Ellman's reagent (5, 5′-dithiobis-(2-nitrobenzoic acid)) in a test tube (0.6 mM). The contents of the mixture were well mixed, and the absorbance was measured at 412 nm using a Shimadzu UV–VIS spectrophotometer within 15 min (UV PC-1600, Japan). The lowered GSH concentration was measured in nanomoles per milligram of protein.

#### 2.3.4. Evaluation of superoxide dismutase (SOD) levels

We used a standard approach to assess the amount of superoxide dismutase (SOD) [49]. In a nutshell, 2.86 mL of tris-buffer (50 mM, pH 8.5) and 0.1 mL of EDTA solution were combined. The reaction mixture was then added to 0.02 mL of homogenate sample and 0.02–0.08 mL of pyrogallol. With the use of a Shimadzu UV PC-1600 spectrophotometer (Japan), the mixture's absorbance was measured at 420 nm against a blank, and the findings were represented in units per mg of protein.

#### 2.3.5. Evaluation of catalase (CAT) levels

The catalase (CAT) enzyme activity was tested using hydrogen peroxide as a substrate, as described by Mondal et al. [49]. The reaction was begun by adding 1 mL of $H_2O_2$ (30 m/mL) to 0.1 mL of homogenate sample and 1.9 mL of PBS (pH 7.0) in a 3 mL cuvette, according to this procedure. The absorbance at 240 nm was measured using a Shimadzu UV PC-1600 UV–VIS spectrophotometer (Japan). The CAT results were given in units per mg of protein.

### 2.4. Histopathological evaluation

Liver tissues were fixed in 10 % neutral buffered formalin for histological examinations. With the use of a rotary microtome (HM 325, Thermo Scientific, U.K.), liver tissue was cut to a thickness of 5 m and embedded in paraffin wax. Tissue slices were then stained with hematoxylin and eosin and photographed with an Olympus DP 72 microscope (Tokyo, Japan) [39].

### 2.5. In-silico study

After reviewing the literature on identified chemical compounds from the methanolic extract of *P. chaba* stem bark, we selected four bioactive compounds that act on several liver injuries in order to predict their inhibitory activities against CYP2E1 to eventually describe that *P. chaba* may exhibit hepatoprotective activity against APAP-induced liver injury. We downloaded the 3D structure of each compound in structure-data file (SDF) format from the PubChem database and the target protein CYP2E1 (PDB ID 3E6I) was retrieved from the Protein Data Bank (PDB) [50]. With the aid of PYMOL (version 2.5), the protein structure was visualized and all water molecules were eliminated from

the protein structure. Through energy reduction, vacant atomic gaps and crystallographic disturbances were addressed using a *Swiss* PDB viewer v4.1.0. Finally, the ".pdb" format was used to save the improved protein structure [51].

In silico molecular docking with AutoDock vina (version 4; The Scripps Research Institute, La Jolla, CA, USA) on the PyRx platform was used to determine the proper binding modes of the ligands with the targeted protein [52]. After molecular docking, the binding of the bioactive compounds with the amino acid residues of the binding site was visualized in BIOVIA Discovery Studio Visualizer v20.1.0 [53]. The conformations of the best-docking score achieved from docking were further scrutinized for evaluating the stability of the binding mode in the target active site, detailed interactions between the ligand and protein, and their thermodynamic behavior using molecular dynamics (MD) simulation studies [54].

Molecular dynamics simulation, in particular, is of vital interest to researchers in the field of computational drug discovery [55,56]. Thus, molecular dynamics simulation provides an investigation into conformational stability for protein-ligand complexes [57]. Like any technology, molecular dynamics simulation consists of a set of standard protocols. We implemented here those standard protocols to investigate the binding impact of silibinin and piperine on CYP2E1 (PDB ID: 3E6I) [58], with the Charmm 27 force field for all atoms [59]. For the first step of molecular dynamics, the topologies of ligands were generated via Swiss PARAM [60]. The holo forms of CYP2E1 were placed and centered in cubic cell units with at least 0.2 nm distance from the box edges. We chose TIP3P (three-point transferable intermolecular potential) as the solvent for our ligand-bound protein complexes [1,61]. And the charges were adjusted via adding the complexes either sodium ion or chloride ion. In the following step, minimization for systems was done via using the steepest descent algorithm threshold value of 1000 kJ/mol nm. Then, both of the NVT and NPT ensembles of 0.1 ns were used with the position constraint on the protein molecules for controlling pressure at 1 atm and temperature at 300 K [62]. In the next step, to assess the impact of electrostatic interactions on the diversified behaviors of complexes, we utilized the Particle Mesh Ewald summation [63]. We executed 80-ns MD simulation for all systems in the final step. The total processes were done under restraint-free molecular dynamic simulation conditions on protein molecules or ligands to assess stability to this end. MD trajectories were analyzed via employing the RMSD, RMSD of ligands, RMSF, Rg, SASA, and hydrogen bonding. PCA was also analyzed.

### 2.6. Statistical analysis

Results are expressed as the mean ± standard error of the mean (SEM). SPSS (Statistical Packages for Social Science, version 20.0, IBM Corporation, New York, United States of America) and Microsoft Excel 2013 were used to analyze the data (Redmond, Washington, U.S.A.). Data were subjected to one-way analysis of variance (ANOVA), and statistical analysis was performed with the aid of Dunnett's and Tukey's multiple comparison to analyze data sets. Differences were considered significant at 0.1 % and 5 % levels of significance at $p < 0.001$ and $p < 0.05$, respectively.

## 3. Results

### 3.1. Phytochemical identification through GC–MS analysis

Currently, spectrum matching is used in gas chromatography mass spectrometry (GC–MS) to identify compounds by comparing a query mass spectrum to reference mass spectra in a library [64]. Chemical profiling of *methanol* extract of stem of *P. chaba* showed a total of 31 compounds as illustrated in Fig. 3 that belongs to myriad of chemical classes encountered about 75.6 % of the total run using GC–MS. The identified chemical classes were enriched in fatty acid methyl esters (46.23 %) and alkaloids (10.91 %). Piperine is the major components of the extract. Phytol, a diterpene alcohol and pellitorine fatty amide represented 7.53 and 4.76 %, respectively also counted as major component of the extract. Other minor classes of alkanes, volatile terpenes and miscellaneous classes recorded 2.04, 1.81 and 2.31 %, respectively. All the methanol chemical components, their relative percentile and retention time were summarized in Table 1.

### 3.2. Effects of paracetamol, P. chaba stem methanol extract, and silymarin on body weights and relative liver weights

Table 2 shows the effects of *P. chaba* stem methanol extract on body weights and relative liver weights. The rats in the paracetamol-treated negative control group displayed a significant decrease in body weight and relative liver weight as compared to the normal control animals. The treatment groups that were given *P. chaba* stem methanol extract, on the other hand, showed a substantial improvement in body mass and relative liver weight compared to the negative control rats in a dose-dependent manner.

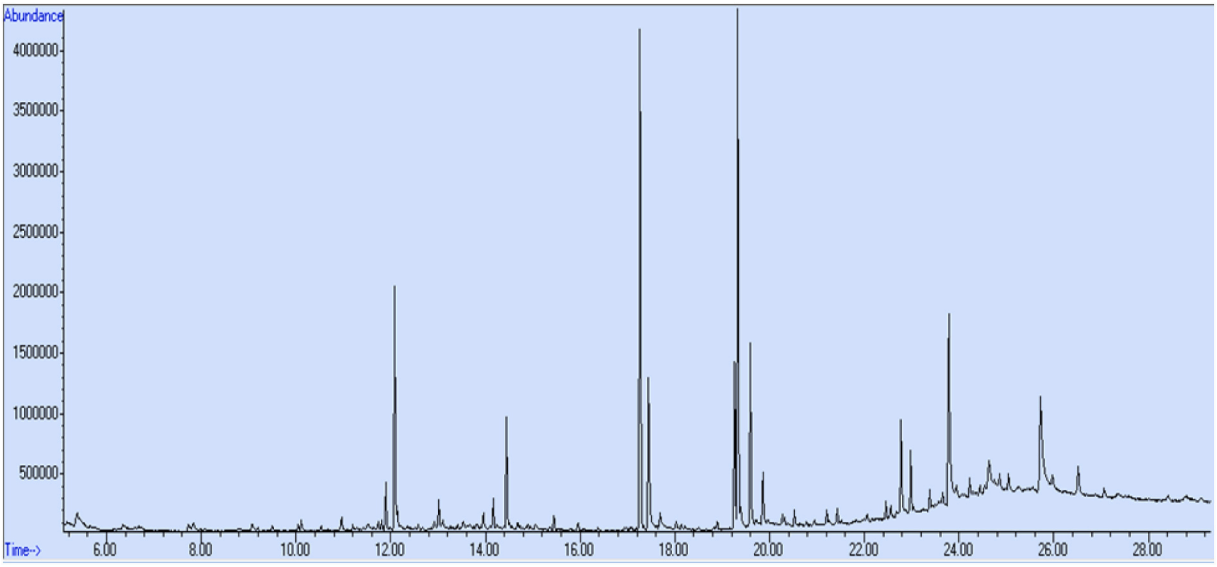


**Fig. 3.** GC–MS total run of methanol extract of *Piper chaba*.

**Table 1**
Total identified compounds of methanol extract of *Piper chaba* using GC–MS.

| Peak no. | Rt. (min) | % area | Compound name | Chemical formula | Chemical class |
|---|---|---|---|---|---|
| 1 | 5.42 | 1.15 | D-Limonene | $C_{10}H_{16}$ | Monoterpene |
| 2 | 6.36 | 0.15 | Benzoic acid methyl ester | $C_8H_8O_2$ | Organic ester |
| 3 | 9.5 | 0.2 | Decanoic acid methyl ester | $C_{12}H_{24}O_2$ | Fatty acid methyl ester |
| 4 | 10.53 | 0.12 | *n*-Tetradecane | $C_{14}H_{30}$ | Hydrocarbon |
| 5 | 10.96 | 0.45 | *β*-Caryophyllene | $C_{15}H_{24}$ | Sesquiterpenes |
| 6 | 11.52 | 0.26 | 2-Butylquinoline | $C_{13}H_{15}N$ | Quinolines |
| 7 | 11.74 | 0.21 | *β*-Cubebene | $C_{15}H_{24}$ | Sesquiterpenes |
| 8 | 11.8 | 0.24 | *n*-Pentadecane | $CH_3(CH_2)_{13}CH_3$ | Alkanes |
| 9 | 11.9 | 1.09 | 2,4-Di-*t*-butyl phenol | $C_{14}H_{22}O$ | Phenol |
| 10 | 12.08 | 5.22 | Dodecanoic acid methyl ester | $C_{13}H_{26}O_2$ | Fatty acid methyl ester |
| 11 | 12.14 | 0.6 | Eicosanoic acid methyl ester | $C_{21}H_{40}O_3$ | Fatty acid methyl ester |
| 12 | 13.02 | 0.69 | *n*-Hexadecane | $C_{16}H_{34}$ | Hydrocarbon |
| 13 | 13.68 | 0.24 | 3,5-Dimethyloctane | $C_{10}H_{22}$ | Alkanes |
| 14 | 13.84 | 0.21 | *n*-Tetratriacontane | $C_{30}H_{62}$ | Alkanes |
| 15 | 14.17 | 0.67 | *n*-Heptadecane | $C_{17}H_{36}$ | Alkanes |
| 16 | 14.44 | 2.52 | Tetradecanoic methyl ester | $C_{15}H_{30}O_2$ | Fatty acid methyl ester |
| 17 | 14.68 | 0.22 | *n*-Eicosane | $C_{20}H_{42}$ | Alkanes |
| 18 | 15.46 | 0.35 | *n*-Octadecane | $C_{18}H_{38}$ | Alkanes |
| 19 | 17.27 | 12.07 | Hexadecanoic acid methyl ester | $C_{17}H_{34}O_2$ | Fatty acid methyl ester |
| 20 | 17.45 | 4.76 | Pellitorine | $C_{14}H_{25}NO$ | Fatty amide |
| 21 | 17.69 | 0.94 | Palmitic acid | $C_{16}H_{32}O_2$ | Fatty acid |
| 22 | 18.14 | 0.11 | Cycloeicosane | $C_{20}H_{40}$ | Alkanes |
| 23 | 18.9 | 0.27 | Indoxol | $C_{22}H_{19}NO_2$ | Indole alkaloid |
| 24 | 19.26 | 3.68 | Linoleic acid methyl ester | $C_{19}H_{34}O_2$ | Fatty acid methyl ester |
| 25 | 19.33 | 12.5 | Oleic acid methyl ester | $C_{19}H_{36}O_2$ | Fatty acid methyl ester |
| 26 | 19.59 | 4.48 | Stearic acid methyl ester | $C_{19}H_{38}O_2$ | Fatty acid methyl ester |
| 27 | 19.86 | 1.8 | N-(2,4-Decadienoyl) piperidine | $C_{15}H_{25}NO$ | Piperidine alkaloid |
| 28 | 21.21 | 1.24 | cis-11-Eicosenoic acid methyl ester | $C_{21}H_{40}O_2$ | Fatty acid methyl ester |
| 29 | 22.78 | 2.78 | 13-Docosenoic acid methyl ester | $C_{23}H_{44}O_2$ | Fatty acid methyl ester |
| 30 | 23.78 | 7.53 | Phytol | $C_{20}H_{40}O$ | Diterpene alcohol |
| 31 | 24.64 | 8.84 | Piperine | $C_{17}H_{19}NO_3$ | Alkaloid |
| Volatiles terpenes | | | | 1.81 | |
| Fatty acid methyl esters | | | | 46.23 | |
| Alkanes | | | | 2.04 | |
| Alkaloids | | | | 10.91 | |
| Diterpene alcohol | | | | 7.53 | |
| Fatty amide | | | | 4.76 | |
| Miscellaneous | | | | 2.31 | |
| Total % | | | | 75.59 | |

### 3.3. Effects of paracetamol, P. chaba stem methanol extract, and silymarin on biochemical parameters

The effects of paracetamol, *P. chaba* stem methanol extract, and standard silymarin on serum hepatic diagnostic markers are displayed in the table below. The use of paracetamol alone increased the levels of blood hepatic enzymes such as ALT, AST, ALP, GGT, and LDH in the negative control group. On the other hand, co-administration of a methanol extract of *P. chaba* stem significantly reduced the levels of these serum enzymes in a dose-dependent manner, as did the standard group (Table 3).

Serum TB, TP, ALB, and GLB, like serum hepatic enzymes, are important indicators for assessing hepatic function. When compared to the vehicle-treated rats, paracetamol therapy significantly increased blood total bilirubin (TB) and globulin (GLB) levels, while co-treatment with stem extract of *P. chaba* amended these levels in a dose-dependent way. The negative control (paracetamol) group, on the other hand, saw a significant decrease in serum total protein (TP) and albumin (ALB). In *P. chaba* stem methanol extract and silymarin, these biochemical parameters were recovered to near-control values (Table 4).

Paracetamol treatment resulted in a substantial ($p < 0.001$) rise in blood TC, TG, and LDL levels, as well as a decrease in HDL values. The

**Table 2**
Effects of paracetamol, *P. chaba* stem methanol extract, and silymarin on body weights and relative liver weights.

| Parameter | Group | | | | |
|---|---|---|---|---|---|
| | Normal control | Negative control | Treatment Group I | Treatment Group II | Standard group |
| Initial body weight (g) | 150.75 ± 12.66 | 150.32 ± 5.79 | 158.50 ± 9.87 | 154.00 ± 9.83 | 160.75 ± 8.49 |
| Final body weight (g) | 173.75 ± 11.33 | 158.27 ± 6.63 | 172.82 ± 8.89 | 176.75 ± 8.82 | 179.25 ± 8.67 |
| Body weight gain (g) | 17.50 ± 2.46 | 7.05 ± 1.01 [a] | 13.50 ± 1.93 | 22.75 ± 1.97 [x] | 18.50 ± 1.44 |
| Liver weight (g) | 5.32 ± 0.18 | 8.58 ± 0.35 [b] | 6.94 ± 0.26 [a, x] | 5.66 ± 0.06 [y] | 5.83 ± 0.37 [y] |

Values are mean ± SEM (n = 7); Significant at $^{a}p < 0.05$, $^{b}p < 0.01$ when compared to normal control. Significant at $^{x}p < 0.05$, $^{y}p < 0.01$ when compared to negative control group.

**Table 3**
Effects of paracetamol, *P. chaba* stem methanol extract, and silymarin on serum hepatic marker enzymes.

| Parameter | Group | | | | |
|---|---|---|---|---|---|
| | Normal control | Negative control | Treatment Group I | Treatment Group II | Standard group |
| ALT (U/L) | 69.03 ± 4.07 | 138.30 ± 5.45$^{b}$ | 99.27 ± 3.45$^{a,x}$ | 82.48 ± 6.16$^{y}$ | 76.50 ± 5.48$^{y}$ |
| AST (U/L) | 123.15 ± 3.03 | 203.07 ± 7.52$^{b}$ | 147.75 ± 5.01$^{a,x}$ | 131.75 ± 5.07$^{y}$ | 127.25 ± 8.53$^{y}$ |
| ALP (U/L) | 195.42 ± 7.42 | 324.25 ± 8.64$^{b}$ | 265.65 ± 8.46$^{b,y}$ | 238.82 ± 7.74$^{a,y}$ | 197.55 ± 5.36$^{y}$ |
| GGT (U/L) | 3.29 ± 0.06 | 6.15 ± 0.09$^{b}$ | 5.64 ± 0.05$^{b,x}$ | 5.02 ± 0.06$^{a,y}$ | 3.96 ± 0.06$^{y}$ |
| LDH (U/L) | 54.16 ± 3.05 | 91.37 ± 4.54$^{b}$ | 66.86 ± 3.43$^{x}$ | 60.48 ± 2.06$^{y}$ | 53.69 ± 3.33$^{y}$ |

Values are mean ± SEM (n = 7); Significant at $^{a}p < 0.05$, $^{b}p < 0.01$ when compared to normal control. Significant at $^{x}p < 0.05$, $^{y}p < 0.01$ when compared to negative control group.

**Table 4**
Effects of paracetamol, *P. chaba* stem methanol extract, and silymarin on TB, TP, ALB, and GLB.

| Parameter | Group | | | | |
|---|---|---|---|---|---|
| | Normal control | Negative control | Treatment Group I | Treatment Group II | Standard group |
| TB (mg/dL) | 0.160 ± 0.009 | 0.223 ± 0.011$^{b}$ | 0.178 ± 0.009$^{x}$ | 0.152 ± 0.006$^{y}$ | 0.160 ± 0.004$^{y}$ |
| TP(g/dL) | 6.20 ± 0.27 | 3.75 ± 0.26$^{b}$ | 4.67 ± 0.13$^{b}$ | 5.48 ± 0.23$^{y}$ | 5.47 ± 0.19$^{y}$ |
| ALB (U/L) | 3.95 ± 0.07 | 2.60 ± 0.17$^{b}$ | 3.08 ± 0.14$^{b}$ | 3.35 ± 0.09$^{a,x}$ | 3.73 ± 0.11$^{y}$ |
| GLB (g/dL) | 1.94 ± 0.09 | 3.10 ± 0.12$^{b}$ | 2.81 ± 0.07$^{b}$ | 2.43 ± 0.05$^{a,x}$ | 2.08 ± 0.07$^{y}$ |

Values are mean ± SEM ($n = 7$); Significant at $^{a}p < 0.05$, $^{b}p < 0.01$ when compared to normal control. Significant at $^{x}p < 0.05$, $^{y}p < 0.01$ when compared to negative control group.

standard silymarin, on the other hand, dramatically ($p < 0.01$) reversed all of these alterations, bringing them back to near-normal control. Similarly, as shown in Table 5, methanol extract of *P. chaba* stem considerably ($p < 0.05$, $p < 0.01$) and dose-dependently reduced paracetamol-induced changes in rats.

### 3.4. Effects of paracetamol, P. chaba stem methanol extract, and silymarin on lipid peroxidation and liver antioxidant enzymes

The effects of paracetamol, *P. chaba* stem methanol extract, and silymarin on the levels of TBARS generated as a consequence of lipid peroxidation in the liver tissue of experimental rats are shown in Fig. 4. When compared to the normal control group, paracetamol-intoxicated rats had significantly higher TBARS levels ($p < 0.01$). The silymarin-treated group, on the other hand, considerably ($p < 0.01$) improved the parameters in the animals. Similarly, when stem extract of *P. chaba* was co-treated with paracetamol, the results showed a significant reduction in TBARS levels, implying that stem extract of *P. chaba* provides hepatocellular protection against paracetamol-induced lipid peroxidation.

Calculating liver endogenous non-enzymatic reduced glutathione (GSH) and enzymatic cellular antioxidant superoxide dismutase (SOD), as well as catalase (CAT), was used to assess hepatic antioxidant activity. Paracetamol administration reduced the levels of these endogenous antioxidants in the experimental animals as compared to the normal control group; however, standard silymarin co-treatment considerably restored their levels. Similarly, in a dose-dependent way, co-administration of *P. chaba* stem methanol extract increased their levels (Fig. 4).

### 3.5. Effects of paracetamol, P. chaba stem methanol extract, and silymarin on histological examination of liver tissue

The typical cellular architecture with a characteristic arrangement of sinusoids line, sinusoidal gaps, and central vein can be seen in the normal control group hepatic tissues (0.05 % tween 80 dissolved in 0.9 % NaCl) (Fig. 5(a)). Paracetamol intoxication, on the other hand, resulted in hepatocyte degeneration, including central and lobular necrosis, inflammatory cell infiltrations, and vascular edematous congestion (Fig. 5(b)). The standard medicine greatly decreased these pathological aberrations in the standard group (Fig. 5(e)). Treatment with *P. chaba* stem methanol extract 250 mg/kg resulted in mild inflammation and necrosis (Fig. 5(d)), whereas treatment with *P. chaba* stem methanol extract 500 mg/kg resulted in significant inflammation, vascular edematous congestion, and inflammatory cell infiltrations (Fig. 5(c)).

**Table 5**
Effects of paracetamol, *P. chaba* stem methanol extract, and silymarin on serum lipid profiles.

| Parameter | Group | | | | |
|---|---|---|---|---|---|
| | Normal control | Negative control | Treatment Group I | Treatment Group II | Standard group |
| TC (mg/dL) | 149.17 ± 3.75 | 184.75 ± 3.72$^{b}$ | 174.08 ± 3.46$^{a}$ | 159.02 ± 3.73$^{x}$ | 148.78 ± 7.69$^{y}$ |
| TG (mg/dL) | 290.18 ± 13.11 | 495.35 ± 20.97$^{b}$ | 358.70 ± 11.96$^{a,y}$ | 312.98 ± 8.09$^{y}$ | 303.59 ± 10.96$^{y}$ |
| LDL-C (mg/dL) | 43.48 ± 4.01 | 98.98 ± 7.12$^{b}$ | 59.34 ± 4.77$^{y}$ | 54.55 ± 2.85$^{y}$ | 50.17 ± 5.20$^{y}$ |
| HDL-C (mg/dL) | 36.13 ± 2.45 | 20.75 ± 2.06$^{b}$ | 30.00 ± 1.47 | 34.25 ± 1.65$^{x}$ | 38.75 ± 2.06$^{y}$ |

Values are mean ± SEM (n = 7); Significant at $^{a}p < 0.05$, $^{b}p < 0.01$ when compared to normal control. Significant at $^{x}p < 0.05$, $^{y}p < 0.01$ when compared to negative control group.

### 3.6. In silico study

Molecular docking of the selected compounds Silibinin, Piperine, Phytol, Pellitorine, and β-caryophyllene with CYP2E1 (PDB ID: 3E6I) was performed, and individually, these compounds showed a binding energy of −9.0, −8.0, −6.2, −6.1, and −6.1, respectively (Table 6). The binding amino acid residues specifically involved in hydrogen bond and hydrophobic interactions are listed in Table 6 and displayed in Fig. 6. The results of MD simulations and PCA analysis are represented in Figs. 7 and 8, respectively.

## 4. Discussion

Although paracetamol (acetaminophen) is widely used as an antipyretic and analgesic, it can induce liver damage if used in excess. Paracetamol is primarily metabolized by the liver into excretable glucuronide and sulfate conjugates [42]. Paracetamol is transformed by cytochrome P450 enzymes (CYPs), chiefly CYP 2E1, to *N*-acetyl-p-benzoquinone imine (NAPQI), a highly reactive metabolite that causes severe respiratory chain dysfunction, reactive oxygen species (ROS) overproduction, c-Jun N-terminal kinase (JNK) activation, mitochondrial permeability transition, and ATP depletion [65]. In vitro studies have indicated that human CYP2E1 is involved in 30–78 % of paracetamol metabolism. The quantity of NAPQI generated in vitro is likewise dramatically reduced when CYP2E1 is inhibited [66]. On the other hand, glutathione protects hepatocytes against covalent attachment to liver proteins by interacting with the reactive metabolite of paracetamol. When phase II metabolizing enzymes are saturated as a result of an APAP overdose, high NAPQI depletes GSH, causing covalent sulfhydryl group attachment in cellular proteins, particularly mitochondrial proteins [67]. This causes mitochondrial oxidative stress and malfunction, which eventually leads to hepatocyte necrosis. As a result, cytochrome induction and glutathione depletion are the primary factors that predispose to liver injury [68].

Hepatic cell damage causes cellular enzymes to seep into the bloodstream, which may then be quantified in the serum. As a result, serum ALT, AST, and ALP values are frequently employed as markers of the severity of liver disease. ALT is a liver enzyme that aids in the metabolism of amino acids and gluconeogenesis [69]. This enzyme catalyzes the transfer of an amino group from alanine to α-ketoglutarate, resulting in glutamate and pyruvate. An increase in AST is frequently followed by a rise in ALT, which is involved in the conversion of amino acids to keto acids [42]. ALP, like other hydrolases, is a member of the hydrolase family, and an increase in this enzyme implies hepatobiliary illness [70]. When compared to the control group, paracetamol administration generated a substantial increase in enzyme levels such as AST, ALT, and ALP, which is consistent with earlier results [12,71]. Because of its preventive action, animals treated with both dosages of *P. chaba* stem methanol extract restored these enzyme levels in the blood, and these findings were corroborated by earlier studies carried out by Yesmin et al. [27]. γ-Glutamyl transferase (GGT), the most important sign of liver disease, is a cell membrane-bound enzyme that catalyzes the γ-glutamyl transfer reaction from peptides to amino acids or other peptides. As demonstrated in the negative control group, membrane permeability produced by paracetamol toxicity increases serum GGT levels, which is consistent with Uchida et al.'s results' [72]. Standard silymarin and *P. chaba* stem methanol extract, on the other hand, reduced serum GGT levels in a dose-dependent manner in the rat liver due to their protective impact. The interconversion of lactate and pyruvate is catalyzed by lactate dehydrogenase (LDH), which is located in the cytoplasm of cells. The release of this enzyme signals that the cellular membrane has opened or that the cell has died [73]. In experimental rats, paracetamol therapy was associated with an increase in serum LDH levels, whereas *P. chaba* stem methanol extract lowered serum GGT levels in a dose-dependent way.

Hepatobiliary disease and severe disturbances in hepatocellular

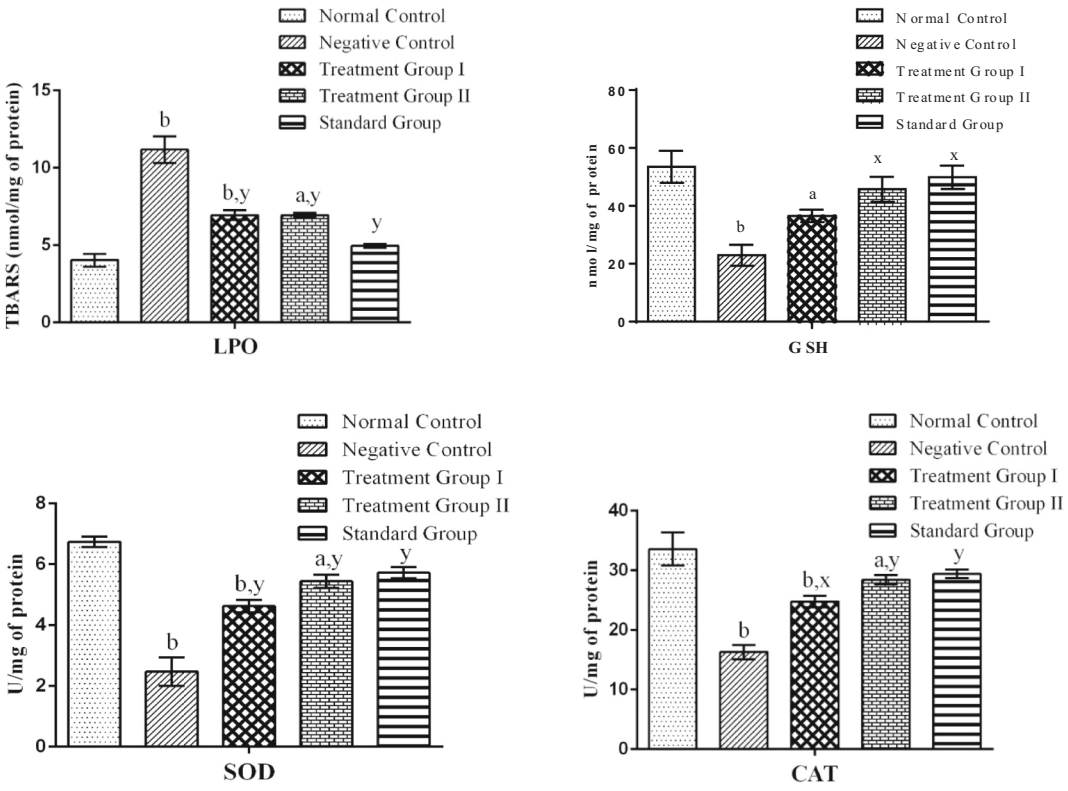


**Fig. 4.** Effects of paracetamol, *P. chaba* stem methanol extract on the hepatic oxidative markers. [Values are mean ± SEM ($n = 7$); Significant at $^{a}p < 0.05$, $^{b}p < 0.01$ when compared to normal control. Significant at $^{x}p < 0.05$, $^{y}p < 0.01$ when compared to negative control group].

function are indicated by a rise in serum total bilirubin, a hepatic function index [74]. The ability of the *P. chaba* stem methanol extract to restore normal liver function after treatment with the extract in liver damage caused by paracetamol was demonstrated by a decrease in serum bilirubin following treatment with the extract in liver damage caused by paracetamol. Similarly, paracetamol administration significantly increased blood globulin levels compared to the normal control group animals, while stem methanol extract of *P. chaba* co-treatment significantly reduced these levels compared to the negative control group rats. The serum total protein and albumin levels of the paracetamol-treated rats were shown to be lower in this study. Hypoalbuminemia is a common symptom of liver illness, and a drop in serum total protein is a reliable indicator of the degree of cellular failure. The severity of hepatopathy was demonstrated by the lowered levels of total protein in paracetamol-treated rats [68]. Increased levels of serum protein and albumin in the *P. chaba* extract pre-treated groups indicate that the liver cells' functional state has improved. One of the most important indicators of liver tissue injury is the lipid profile. By compromising the integrity of the cellular membrane, oxidative stress disrupts lipid metabolism, resulting in the release of certain membrane lipids into the bloodstream [75]. When compared to the normal control group, the paracetamol-treated group showed a substantial rise in serum TC, TG, and LDL-C, as well as a significant drop in serum HDL—C. This finding is consistent with Raghavendran et al., who found that paracetamol-treated rats had higher total cholesterol, triglycerides, and serum LDL-cholesterol levels, as well as lower levels of serum HDL-cholesterol [76,77]. However, treatment with *P. chaba* stem methanol extract caused a decrease in the TC, TG, and LDL-C levels and an increase in HDL-C.

In experimental animals exposed to hazardous toxicants, lipid peroxidation (LPO) is a well-known source of cellular damage, and the initiation of oxidative stress is characterized by an increase in the quantity of thiobarbituric acid reactive substances (TBARS) [78]. Glutathione (GSH), on the other hand, is an endogenous tri-peptide non-enzymatic antioxidant that reduces $H_2O_2$ and scavenges ROS and RNS to protect cells against oxidative stress-mediated cellular damage [79]. Normally, paracetamol's poisonous metabolite NAPQI is conjugated with GSH for detoxification; however, a toxic dose of paracetamol produces a large amount of NAPQI, resulting in fast GSH depletion. When cellular GSH is reduced, poisonous NAPQI binds covalently to cysteine residues in cellular proteins. As a result, a reduced amount of GSH in paracetamol-treated experimental animals is connected to an increase in lipid peroxidation [67]. In the current study, paracetamol treatment resulted in an increase in lipid peroxidation and a depletion of GSH stores. Previous research on paracetamol-induced hepatotoxicity found that GSH levels were reduced and MDA levels were elevated [71]. According to our findings, co-treating paracetamol-exposed rats with *P. chaba* stem methanol extract dramatically replenished GSH and reduced TBARS levels to normal levels.

According to research, SOD is one of the most important enzymes in the enzymatic antioxidant defense system. The superoxide anion is scavenged and converted to hydrogen peroxide, lowering the radical's toxicity. Hepatocellular damage is detected by a decrease in SOD enzyme activity [68]. CAT is an enzymatic antioxidant found in all mammalian organs, with red cells and the liver having the greatest levels of activity. CAT decomposes hydrogen peroxide and protects tissues from highly reactive hydroxyl radicals. A reduction in CAT activity may have a number of detrimental repercussions as a result of the absorption of superoxide radical and hydrogen peroxide [68]. The paracetamol treatment resulted in a drop in these enzyme levels, but the *P. chaba* stem methanol extract treatment resulted in a significant rise in SOD and CAT activity. As a result of our observations, we believe that *P. chaba* stem methanol extract has the ability to inhibit the buildup of excessive free radicals, thus protecting the liver against paracetamol intoxication.

The ability to determine the degree of histo-architectural alterations in hepatocytes requires histopathological investigation [80]. Biochemical findings are substantially confirmed by histopathological

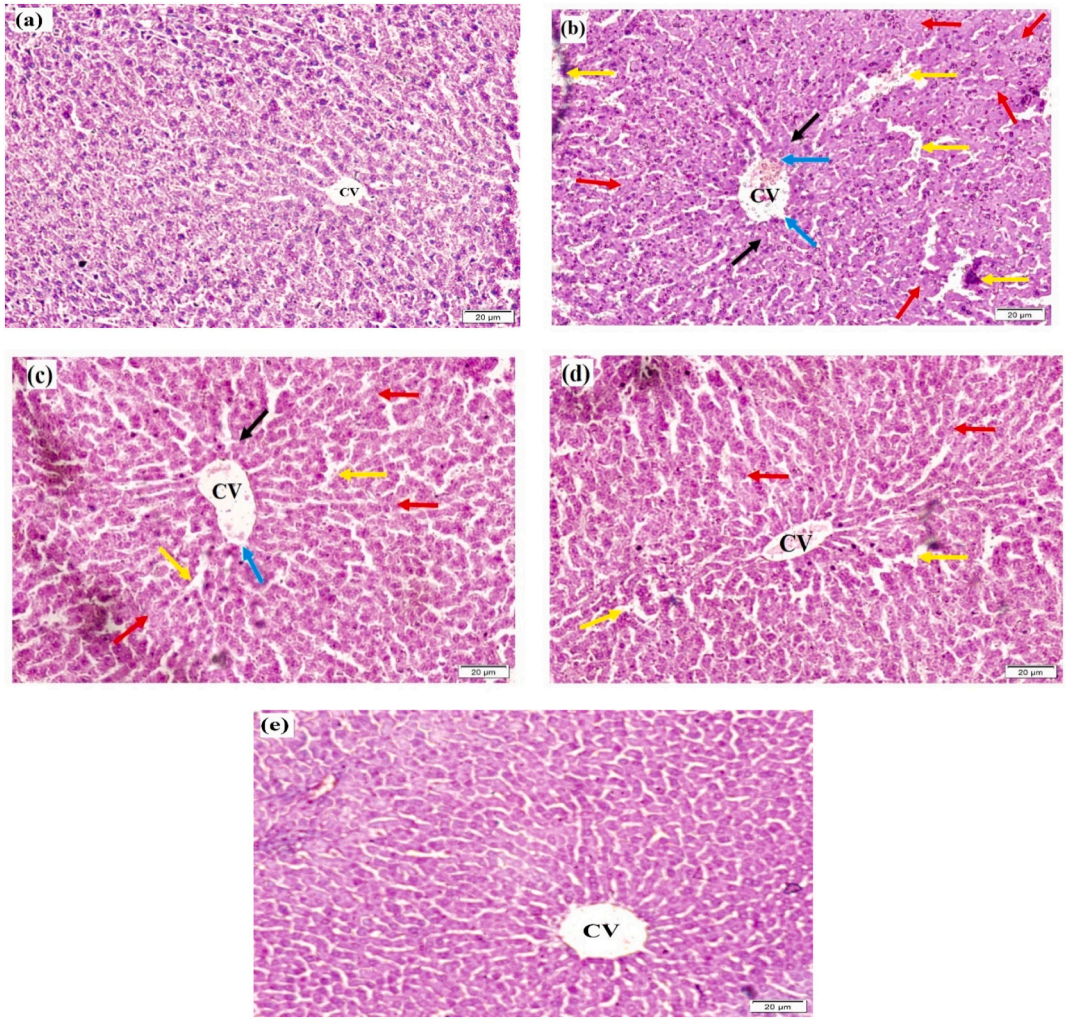


**Fig. 5.** Effects of paracetamol, *P. chaba* stem methanol extract, and silymarin on the histological examination of liver tissue against paracetamol-induced histological changes in investigated animals. (a): Normal control, (b): Negative control, (c): Treatment Group I, (d): Treatment Group II, (e): Standard group. [Magnification: 40×; scale bar: 20 μm]. (The red and yellow arrows denote necrosis in the peripheral area of the central vein and the lobule, respectively, while the blue arrow denotes congestion in the central vein along with extensive inflammatory infiltrates, and the green arrow denotes edema in various locations). (For interpretation of the references to colour in this figure legend, the reader is referred to the web version of this article.)

observations, according to the findings of this investigation. Paracetamol causes hepatocyte degenerative changes, inflammatory cell infiltrations and vascular congestion with edematous spaces by generating reactive oxygen species (ROS). These results are in line with what we've seen in paracetamol-intoxicated rat hepatocytes [81]. Due to inflammatory cell infiltrations, and vascular congestion, liver weight was augmented. The histological section of the rats treated with *P. chaba* stem methanol extract and standard, on the other hand, showed a notable degree of cellular protection by lowering necrosis, inflammatory cell infiltrations, and vascular edema.

From GCMS analysis, the alkaloids class comprised 10.91 % of the total identified chemicals, exemplified by piperine (8.84 %). Piperine is the chief bioactive compound in all piper species [82] that is responsible for the piper's pungent taste and odor. Many previous studies demonstrated that piperine has a variety of pharmacological uses, including antioxidant, anti-inflammatory, anticancer, antimicrobial, adipogenesis, hepato-protective, gastro-protective, anti-diabetic, and immune-modulatory effects [35]. An earlier study revealed the presence of piperine from the stem of *P. chaba* through NMR spectroscopy [83]. Sabina et al. demonstrated that piperine from black pepper has a potent hepatoprotective activity of 25 mg/kg [84]. Piperine was isolated from black and long peppers by Koul and Kapil, who demonstrated hepatoprotective efficacy by reducing tBHP- or $CCl_4$-induced liver damage [85]. According to Morsy et al., piperine's hepatoprotective effects against paracetamol are mediated through antioxidant, anti-inflammatory, and anti-apoptotic capabilities, as well as regulation of transforming growth factor receptor-associated binding protein [86]. Piperine was demonstrated to augment *Boerhaavia diffusa*'s hepatoprotective activity in a dose-dependent way [87]. Another study reveals that piperine co-administration potentiated the hepatoprotective effects of *Aegle miarmelos* against paracetamol-induced hepatotoxicity [88]. Piperine also boosted curcumin absorption in mice, amplifying its protective effects against cognitive impairment and oxidative damage produced by persistent unexpected stress (CUS) [89]. According to Adeyemo et al., piperine reduced oxidative stress, depleted antioxidants, and enhanced liver performance markers induced by Diisononyl phthalate (DINP), and showed protective advantages against hepatotoxicity in rats [90]. Piperine has been discovered to have a possible therapeutic impact on hepatic fibrosis by restoring liver enzymes and targeting the TGF/Smad signaling pathway, as demonstrated by lower TGF-, Smad-3, and miR-17-5p expression levels [91].

Phytol diterpene alcohol, rich in *P. chaba* methanol extract, has already proved its pharmacological efficacy as an antibacterial agent, inhibiting numerous targets of bacterial cells such as *E. coli* and

**Table 6**
Comparative docking scores and noncovalent interactions of four compounds of *P. chaba* with CYP2E1 (PDB ID: 3E6I).

| Ligands | | Docking energy (kcal/mol) | Noncovalent interactions | |
|---|---|---|---|---|
| Name | PubChem CID | | Hydrogen bond | Hydrophobic |
| Silibinin[s] | 31553 | −9.0 | HIS81, LEU471, SER395, THR58, SER472 | PHE360, PRO406, PRO473 |
| Piperine | 638024 | −8.0 | HIS81, SER395, PHE360 | TYR398 |
| Phytol | 5280435 | −6.2 | GLY300, GLY439 | ALA299, ALA438, LIE115, LEU368, VAL364, CYS437, PHE298, PHE478 |
| Pellitorine | 5318516 | −6.1 | CYS480, TYR398 | ILE361, PRO473, HIS81, TYR310, PHE360 |
| β-Caryophyllene | 250139796 | −6.1 | – | ILE115, ALA299, VAL364, LEU368, CYS437, PHE207, PHE298 |

[s] Represents the standard drug.

*Pseudomonas aeruginosa* due to its lipophilic nature. Phytol was shown to be both an antioxidant and a cytotoxic agent, with the cytotoxic impact being mediated via the activation of apoptosis and protective autophagy [92]. In afflicted animals, phytol demonstrated considerable hepatoprotective effects by lowering elevated levels of ALT, AST, ALP, TG, cholesterol, and bilirubin while raising lowered levels of TP, SOD, CAT, and GSH [93]. Phytol can also protect HaCaT keratinocytes from oxidative damage caused by $H_2O_2$ [94]. Abd El-Ghffar et al. extracted phytol from n-hexane extract of Acrocarpus fraxinifolius leaves and found that it has hepatoprotective effects in male albino rats subjected to paracetamol [95]. Phytol had a significant antioxidant effect, eliminating hydroxyl radicals and nitric oxide while also blocking the formation of thiobarbituric acid reactive chemicals (TBARS) [96]. Due to its enrichment in phytol chemical constituents, ethyl acetate extract of *P. betle* demonstrated its anti-quorum sensing and anti-biofilm impact on the nosocomial pathogen *Serratia marcescens* in previous research [97]. Pellitorine, a significant amide alkaloid present in *Piper longum*, *Zanthoxylum caribaeum*, and *Piper mullesua*, was detected in *P. chaba* stem methanol extract by GC–MS analysis in our work [98]. Similarly, pellitorine is one of the primary compounds in *Anacyclus pyrethrum* root extract, and root extract has a potential hepatoprotective effect in experimental rats against isoniazid and rifampicin-induced liver injury [99]. Pellitorine also demonstrated its efficacy as an anti-cancer lead chemical on HL60 and MCT-7 malignant cell lines, whereas pellitorine amide demonstrated its antimalarial action in a prior study [100]. Lee et al. discovered that pellitorine protects the vascular barrier by reducing hyperpermeability, cell adhesion molecule expression, and leukocyte adhesion and migration, suggesting that it might be utilized to treat vascular inflammatory diseases [101].

D-limonene (4-isopropenyl-1-methylcyclohexene) is a monocyclic monoterpene with antioxidant, anti-diabetic, anti-cancer, anti-inflammatory, cardio-protective, gastro-protective, hepato-protective, immune-modulatory, anti-fibrotic, and anti-genotoxic properties [102]. By scavenging lipid alkoxyl and peroxyl radicals and increasing free radicals and iron chelating capacities, Selvanathan et al. revealed that D-limonene protects against Adriamycin (ADR)-induced liver damage or hepatotoxicity [103]. Another research revealed that D-limonene is a strong hepatoprotective compound that rescues the liver against chronic constraint stress-induced injury due to its antioxidant, anti-inflammatory, and anti-apoptotic characteristics [104]. D-antioxidant limonene's antioxidant and anti-inflammatory capabilities, like its hepatoprotective characteristics, can aid in attenuating cardiac injury induced by $CCl_4$ intoxication [105]. We detected β-caryophyllene, a sesquiterpene with anti-inflammatory, anti-carcinogenic, and antioxidant properties [106]. In our GC–MS investigation, Kelany and Abdallah found that a combination of silymarin and β -caryophyllene was hepatoprotective, with the capacity to scavenge oxidants, against ketoprofen-induced hepatotoxicity in rats, returning liver enzymes to near-normal levels [107]. Another research found that β-caryophyllene is an effective inhibitor of lipid peroxidation in carbon tetrachloride-induced liver fibrosis, most likely owing to its free radical-scavenging activity on hydroxyl radicals, superoxide anions, and lipid peroxides [108].

Hexadecanoic acid (palmitic acid) methyl ester and oleic acid methyl ester represented the major fatty acids in the methanol extract of *P. chaba* (12.07 and 12.50 %). The results agreed to some extent with a previous work on chemical profiling of methanol extract of Indian *P. betle* leaf stalk. The GC–MS analysis revealed the enrichment of the extract with fatty acids, mainly hexadecanoic acid methyl ester (16.25 %) [109]. Fatty acids methyl esters viz. oleic, stearic, palmitic, linoleic and linolenic acids reported previously as antioxidant and antifungal agents [110] whereas those fatty acids counted in the chemical profiling of methanol extract of *P. chaba* with variable percentile as shown in Table 1. In another previous work, the hexadecanoic acid methyl ester enriched in clove ethanolic extract proved its efficacy as a potent antibacterial agent against multidrug resistance strains viz. *Pseudomonas aeruginosa*, *Klebsiella pneumonia* and *Staphylococcus aureus* [111], whereas the dichloromethane extract of *P. nigrum* seeds proved its antimicrobial effect against Gram positive *Bacillus subtilis* as well as *Aspergillus niger* fungi [112].

Because the primary oxidation pathway for paracetamol is cytochrome P450, namely CYP2E1, it sets off a chain of events that leads to hepatotoxicity. Several investigations have also demonstrated that paracetamol overdose causes overexpression of the cytochrome P450 CYP2E1 gene [113]. Several earlier studies have shown that blocking the cytochrome CYP450 system protects experimental animals from acetaminophen-induced hepatotoxicity. For instance, rosmarinic acid reduced hepatic CYP2E1 activity and lipid peroxidation while protecting glutathione levels from acetaminophen-induced oxidative stress. [114]. Similarly, *Caralluma umbellata* methanolic extract's hepatoprotective benefits against paracetamol toxicity can be attributed to a combination of antioxidant capabilities and lower CYP2E1 expression [113]. According to Khelfallah and colleagues, *Origanum floribundum* demonstrated hepatoprotective activity against acetaminophen toxicity, in part owing to inhibition of CYP2E1 and NF-B gene expression [115]. Furthermore, diallyl disulfide's protective benefits may be owing to its capacity to reduce acetaminophen metabolic activation by blocking CYP2E1 [116]. Like in vivo studies, an earlier in-silico study has shown that -D-glucopyranosyl inhibits the CYP2E1 protein, resulting in a decrease in the formation of ROS, which helps to alleviate acute paracetamol-induced oxidative stress and liver damage [50].

Therefore, molecular docking studies are now often utilized to predict ligand-target interactions and determine the biological activity of natural products. It not only tells us about the possible mechanism of action of a protein or enzyme, but also about the binding moods inside the binding site [117]. So, we conducted a molecular docking investigation to better understand the interactions between the selected four compounds of *P. chaba* and the target enzyme by revealing their interactions on the human CYP2E1 (PDB ID: 3E6I) active site (Table 1). Among all the four ligands, piperine exhibited the highest interaction with CYP2E1 (−8.0 kcal/mol) and visualized a higher number of hydrogen bonds ($n = 3$) interacting with HIS81, SER395, and PHE360 amino acid residues of the selected target. The binding affinity and hydrogen interaction between ligands and target protein were compared with standard drug silibinin.

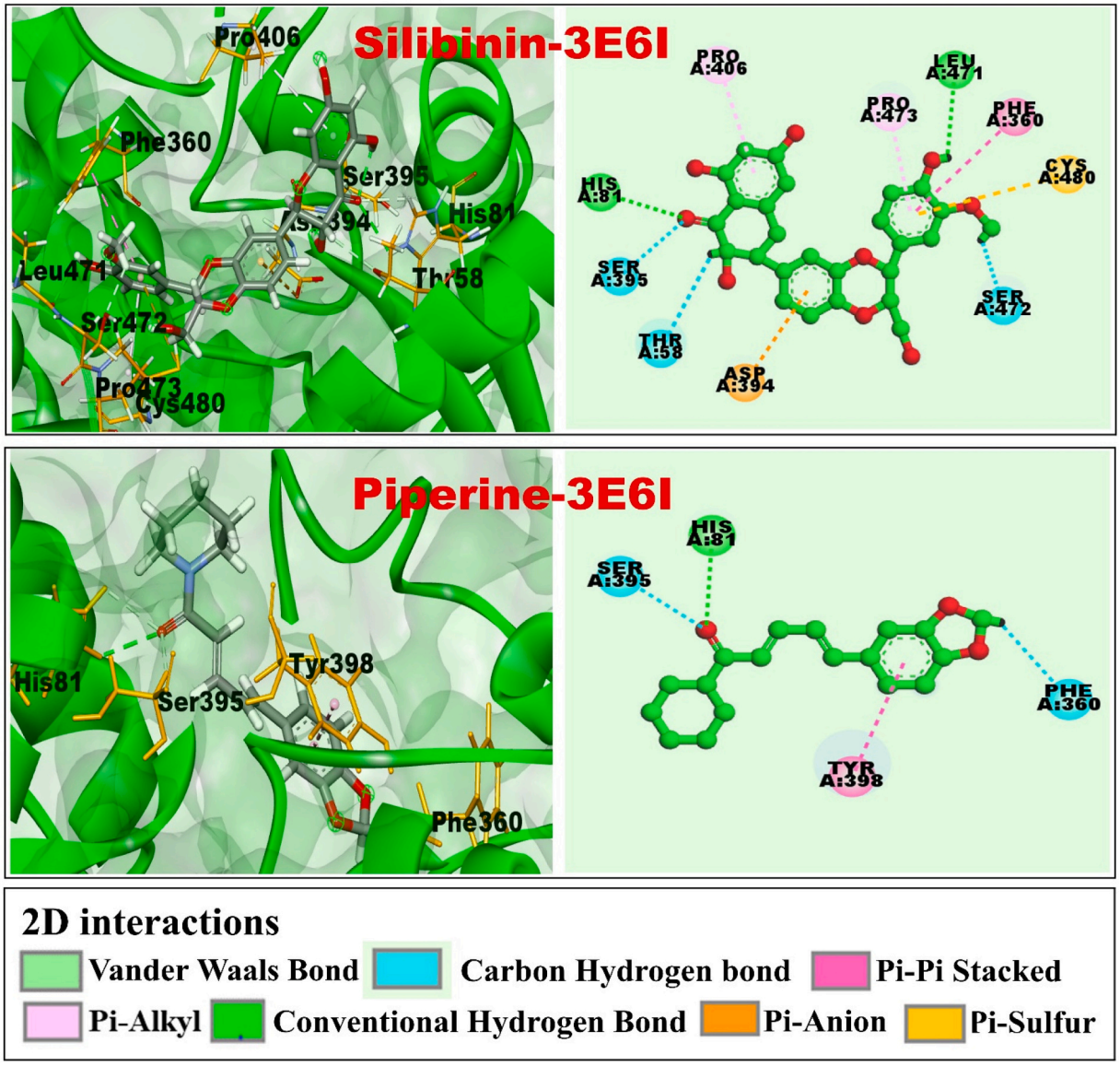


**Fig. 6.** Nonbonding interaction of silibinin and piperine with target CYP2E1 (PDB ID: 3E6I).

Silibinin, the primary ingredient of silymarin, a flavonoid medicine derived from the *Silybum marianum* plant that is used to treat liver illness, was examined for its ability to inhibit human CYP450 enzymes, especially CYP2E1 [50,118]. Silymarin, a flavolignan derived from this plant's fruits and seeds, has been shown to protect against cirrhosis, jaundice, and hepatitis [119]. Furthermore, in vitro, in vivo, and clinical investigations have shown that silymarin and its main active ingredient silibinin (silybin), a polyphenolic compound, exhibit antioxidant and hepatoprotective properties in animal and human models of alcoholic and nonalcoholic chronic liver disorders (Haddad et al., 2011). The binding energy of silibinin to CYP2E1 is −9.0 kcal/mol, and silibinin connected with the active site cavity via hydrogen bonding interactions with HIS81, LEU471, SER395, THR58, and SER472.

During the molecular docking analysis, we found that piperine interacted with a very similar number of active amino acid residues present in the active cavity of the enzyme with hydrogen bond interacting forces and parallel interaction energy as compared to silibinin. The binding energy of piperine-3E6I complex is very close to the binding energy of silibinin-3E6I complex. On the other hand, the number of hydrogen bond interactions of piperine-3E6I is nearly similar to the silibinin-3E6I complex (Fig. 3). After analyzing this docking study, it is clear that the activity of piperine against APAP-induced hepatotoxicity through targeting CYP2E1 is closely related to that of the silibinin. Finally, we selected the best complex structure found as the best pose among all conformers with the lowest docking interaction energy (kcal/mol) of −8.0 (piperine).

The structure of the best-docked conformation of piperine achieved from docking in a complex with 3E6I was further scrutinized to evaluate the stability of the binding mode in the target active site, detailed interactions between the ligand and protein, and their thermodynamic behavior using molecular dynamics (MD) simulation studies.

In short, understanding the dynamics and interactions of ligand–protein is crucial to the drug discovery process. RMSD analysis is used to understand the dynamical behavior of studied complexes [56]. Fig. 4A compares the RMSD between the impact of silibinin and piperine on CYP2E1 dynamical fluctuations. From Fig. 7(a) there is a clear trend of decreasing RMSD values' averages of CYP2E1 protein when it bound to silibinin and overall average for RMSD is 0.14674 nm whereas the overall average for piperine is 0.17833 nm. Moving on now to consider the dynamics of silibinin and piperine inside the binding site of CYP2E1 via measuring the RMSD for silibinin's and piperine's atoms (Fig. 7(b)). From this data, we can see that the RMSD for silibinin resulted in a lower

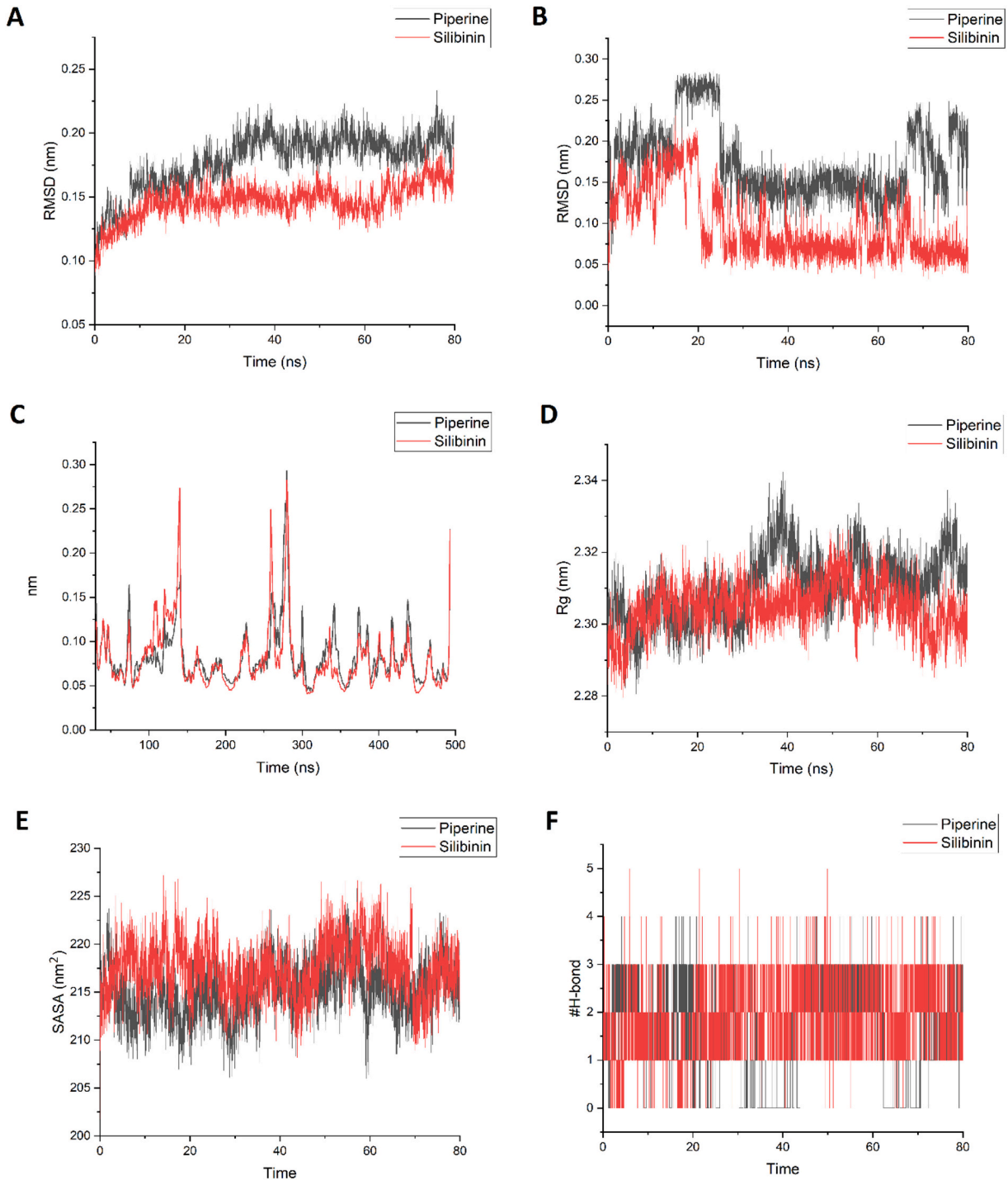


**Fig. 7.** MD simulations analysis (a) RMSD for backbone atoms of CYP2E1 protein, (b) RMSD for ligands' atoms, (c) RMSF for backbone atoms of CYP2E1 protein, (d) Rg for 6 LU7 protein, (e) SASA for CYP2E1 and (f) Hydrogen bonding of ligands with CYP2E1 protein.

fluctuation than piperine during 80 ns.

Another important key of MD simulation is the residual flexibility of a protein's backbone, which can be investigated via the RMSF value. The RMSF values were calculated to investigate the effect of silibinin and piperine on the residual flexibility of the CYP2E1 backbone (Fig. 7(c)). The lower average RMSF values were for silibinin (0.079359307 nm) than for piperine (0.082403896 nm).

For deep examination about the impact of selected ligands, we studied the radius of gyration (Rg) of the all holo CYP2E1 systems (Fig. 7 (d)). The resulting Rg values for CYP2E1-silibinin more compactness. We also analyzed the SASA values for CYP2E1-silibinin and CYP2E1-piperine as shown in Fig. 4E. From this figure, the SASA values were 215.1154508 and 217.4705999 for piperine and silibinin, respectively. Further, the strength of interactions of piperine and silibinin with CYP2E1 assessed via estimating the hydrogen bonds during the 80 ns (Fig. 7(f)). The number of hydrogen bonds was 1.442944632 and 1.872140982 for piperine and silibinin, respectively.

The PCA analysis for backbone atoms of holo CYP2E1 systems was assessed for the obtained MD trajectories. Fig. 8. Where PC1 and PC2 were plotted together to show the essential dynamics of collective motion. It can be seen there is insignificant change between the piperine and silibinin on the essential dynamics of CYP2E1 but the PCA for

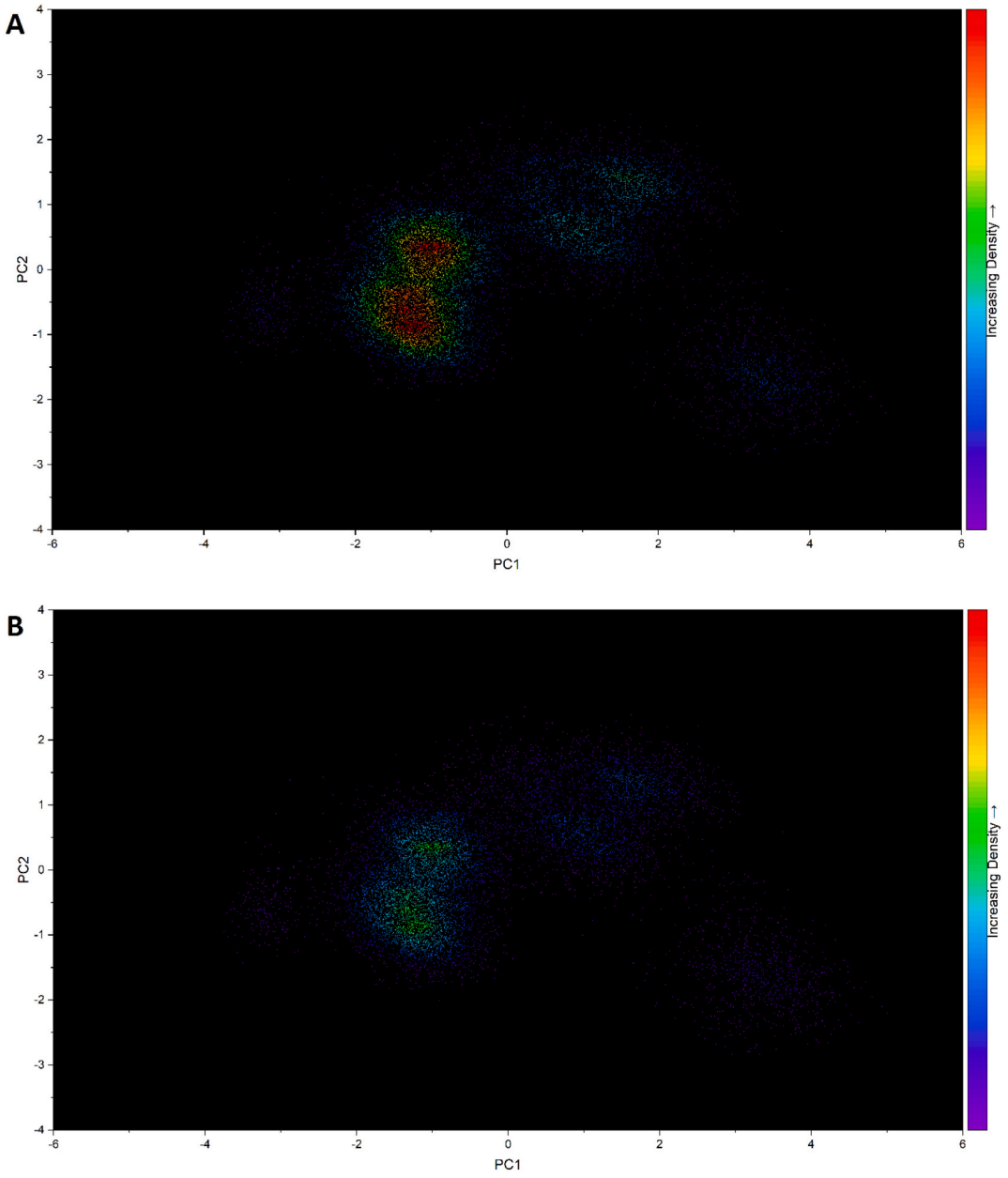


**Fig. 8.** PCA analysis (a) for backbone atoms of piperine–bound CYP2E1 protein and (b) for backbone atoms of silibinin–bound CYP2E1 protein.

CYP2E1- piperine is a larger than CYP2E1- silibinin. The quantitative analysis of the overall flexibility of piperine–bound CYP2E1 and silibinin–bound CYP2E1 was determined via a trace of the diagonalized covariance matrix. The traces of the covariance matrix values were 10.8545 and 10.4341 for piperine and silibinin, respectively.

In addition, like silibinin, piperine significantly reduced the RMSD values for the backbone atoms of CYP2E1. Also, the RMSD values for piperine atoms were closely similar to those for silibinin. Moreover, the hydrogen bonding analysis showed that piperine also binds strongly to CYP2E1 as like silibinin and thereby the PCA and diagonalized covariance matrix values for piperine–bound CYP2E1 indicate that CYP2E1 is more restricted.

In summary, *P. chaba* stem bark extract is high in fatty acid methyl esters (46.23 %) and alkaloids (10.91 %), according to the GC–MS study, and piperine is identified as a key phytochemical. Piperine (−8.0 kcal/mol) was discovered to interact and be more stable with the binding site of CYP2E1 than any of the other identified phytochemicals. The administration of *P. chaba* amended the anomalies and improved the histo-architectural arrangement of hepatocytes in treated groups. This extract also inhibited the alteration of endogenous antioxidant enzymes and MDA levels as compared to the paracetamol treated group and returned them to their normal state. We may thus infer from all of our data that the *P. chaba* stem extract's primary ingredient, piperine, has the ability to counteract hepatic damage by APAP.

## 5. Conclusion

In conclusion, by evaluation of the in vivo hepatoprotective activity of the methanolic extract of *P. chaba*, it has been revealed that co-administration of *P. chaba* at both doses with APAP significantly ameliorated APAP-induced acute liver injury by enhancing anti-oxidative defenses and accelerating APAP harmless metabolism, inhibiting the formation of hepatotoxic intermediated NAPQI and hepatic release of cytokines to enhance the levels of phase II enzymes, which was verified with the improvement of APAP-induced distress in oxidative stress in rat liver by reducing the activities of CAT, SOD, and GSH as well

as serum albumin, globulin, hepatic enzymes, histopathological architecture, lipid profiles, total protein, and total bilirubin and elevating the MDA level. The GC–MS analysis indicated the presence of many components in this extract, some of which have been shown to have hepatoprotective properties. In in silico screening, piperine, among the identified compounds from the extract of *P. chaba*, has been found the most effective compound against liver injury by targeting CYP2E1 through molecular docking study and MD simulation. However, more investigations (pre-clinical and clinical studies) are needed to determine the safety and efficacy of *P. chaba* extract as a therapeutic intervention for drug or toxicant-induced liver impairment.

## CRediT authorship contribution statement

Chandan Sarkar - Conceptualization.
Milon Mondal - Conceptualization.
Khattab Al-Khafaji - Methodology.
Dina M. El-Kersh - Methodology.
Sarmin Jamaddar - Methodology.
Pranta Ray - Experimental.
Uttam Kumar Roy - Experimental.
Mirola Afroze - Experimental.
Md. Moniruzzaman - Software/statistics.
Mala Khan - Software/statistics.
Umma Hafsa Asha - First draft of the manuscript.
Abul Bashar Ripon Khalipha - First draft of the manuscript.
Edna Mori - Resources.
Bruna Caroline Gonçalves Vasconcelos de Lacerda - Resources.
Isaac Moura Araújo - First draft of the manuscript.
Henrique Douglas Melo Coutinho - Project administration.
Muhammad Torequl Islam - Supervision.

## Declaration of competing interest

The authors declare that they have no known competing financial interests or personal relationships that could have appeared to influence the work reported in this paper.

## Data availability

Data will be made available on request.

## References


[1] M. Hasan, A.A. Khan, Development of gastroenterology in Bangladesh, J. Gastroenterol. Hepatol. 12 (1997) S13–S14, https://doi.org/10.1111/j.1440-1746.1997.tb00437.x.

[2] M.S. Al-Said, R.A. Mothana, M.M. Al-Yahya, S. Rafatullah, M.O. Al-Sohaibani, J. M. Khaled, A. Alatar, N.S. Alharbi, M. Kurkcuoglu, H.C. Baser, GC-MS analysis: in vivo hepatoprotective and antioxidant activities of the essential oil of Achillea biebersteinii Afan. growing in Saudi Arabia, Evid. Based Complement. Alternat. Med. 2016 (2016) 1–8, https://doi.org/10.1155/2016/1867048.

[3] B. Ellahi, A.M. Salman, S.A. Sheikh, E. Summra, Hepatoprotective and hepatocurative properties of alcoholic extract of Carthamus oxyacantha seeds, Afr.J. Plant Sci. 8 (2014) 34–41, https://doi.org/10.5897/AJPS12.053.

[4] B.R. Galani, B.A. Owona, D.P. Chuisseu, E. Machewere, C.B. Ngantchouko, P. F. Moundipa, Hepatoprotective activity of Leptadenia hastata (asclepiadaceae) on acetaminophen-induced toxicity in mice: in vivo study and characterization of bioactive compounds through molecular docking approaches, Biomed. Res. Int. 2020 (2020), https://doi.org/10.1155/2020/3807234.

[5] A. Omidi, N. Riahinia, M.B.M. Torbati, M.-A. Behdani, Hepatoprotective effect of Crocus sativus (saffron) petals extract against acetaminophen toxicity in male Wistar rats,Avicenna, J. Phytomedicine 4 (2014) 330.

[6] N. Kanwal, A. Rasul, G. Hussain, H. Anwar, M.A. Shah, I. Sarfraz, A. Riaz, R. Batool, M. Shahbaz, A. Hussain, Z. Selamoglu, Oleandrin: a bioactive phytochemical and potential cancer killer via multiple cellular signaling pathways, Food Chem. Toxicol. 143 (2020), 111570, https://doi.org/10.1016/j.fct.2020.111570.

[7] M. Blieden, L.C. Paramore, D. Shah, R. Ben-Joseph, A perspective on the epidemiology of acetaminophen exposure and toxicity in the United States, Expert. Rev. Clin. Pharmacol. 7 (2014) 341–348, https://doi.org/10.1586/17512433.2014.904744.

[8] J.A. Hinson, D.W. Roberts, L.P. James, Mechanisms of acetaminophen-induced liver necrosis, Adverse Drug React. (2010) 369–405, https://doi.org/10.1007/978-3-642-00663-0_12.

[9] N. Azarmehr, P. Afshar, M. Moradi, H. Sadeghi, H. Sadeghi, B. Alipoor, B. Khalvati, Z. Barmoudeh, K. Abbaszadeh-Goudarzi, A.H. Doustimotlagh, Hepatoprotective and antioxidant activity of watercress extract on acetaminophen-induced hepatotoxicity in rats, Heliyon 5 (2019), e02072, https://doi.org/10.1016/j.heliyon.2019.e02072.

[10] İ.Ö. Aycan, A. Tüfek, O. Tokgöz, O. Evliyaoğlu, U. Fırat, G.Ö. Kavak, H. Turgut, M.U. Yüksel, Thymoquinone treatment against acetaminophen-induced hepatotoxicity in rats, Int. J. Surg. 12 (2014) 213–218, https://doi.org/10.1016/j.ijsu.2013.12.013.

[11] A.H. Tezcan, O. Ozturk, S. Ustebay, Y. Adali, H. Yagmurdur, The beneficial effects of ozone therapy in acetaminophen-induced hepatotoxicity in mice, Pharmacol. Rep. 70 (2018) 340–345, https://doi.org/10.1016/j.pharep.2017.11.003.

[12] Z. Song, C.J. McClain, T. Chen, S-adenosylmethionine protects against acetaminophen-induced hepatotoxicity in mice, Pharmacology 71 (2004) 199–208, https://doi.org/10.1159/000078086.

[13] S. Kalthoff, U. Ehmer, N. Freiberg, M.P. Manns, C.P. Strassburg, Interaction between oxidative stress sensor Nrf2 and xenobiotic-activated aryl hydrocarbon receptor in the regulation of the human phase II detoxifying UDP-glucuronosyltransferase 1A10, J. Biol. Chem. 285 (2010) 5993–6002, https://doi.org/10.1074/jbc.M109.075770.

[14] P. Rada, V. Pardo, M.A. Mobasher, I. García-Martínez, L. Ruiz, A. Gonzalez-Rodriguez, C. Sanchez-Ramos, J. Muntané, S. Alemany, L.P. James, SIRT1 controls acetaminophen hepatotoxicity by modulating inflammation and oxidative stress, Antioxid. Redox Signal. 28 (2018) 1187–1208, https://doi.org/10.1089/ars.2017.7373.

[15] N. Ghosh, R. Ghosh, V. Mandal, S.C. Mandal, Recent advances in herbal medicine for treatment of liver diseases, Pharm. Biol. 49 (2011) 970–988, https://doi.org/10.3109/13880209.2011.558515.

[16] C. Sarkar, S. Jamaddar, T. Islam, M. Mondal, M.T. Islam, M.S. Mubarak, Therapeutic perspectives of the black cumin component thymoquinone: a review, Food Funct. 12 (2021) 6167–6213, https://doi.org/10.1039/D1FO00401H.

[17] C. Sarkar, C. Quispe, S. Jamaddar, R. Hossain, P. Ray, M. Mondal, Z. Abdulwanis Mohamed, M.Sani Jaafaru, B. Salehi, M.T. Islam, A.Faizal Abdull Razis, M. Martorell, E. Pastene-Navarrete, J. Sharifi-Rad, Therapeutic promises of ginkgolide A: a literature-based review, Biomed. Pharmacother. 132 (2020), 110908, https://doi.org/10.1016/j.biopha.2020.110908.

[18] O. Goni, M.F. Khan, Md.M. Rahman, Md.Z. Hasan, F.B. Kader, N. Sazzad, M. A. Sakib, B. Romano, Md.A. Haque, R. Capasso, Pharmacological insights on the antidepressant, anxiolytic and aphrodisiac potentials of Aglaonema hookerianum Schott, J. Ethnopharmacol. 268 (2021), 113664, https://doi.org/10.1016/j.jep.2020.113664.

[19] D. Ağagündüz, T.Ö. Şahin, B. Yılmaz, K.D. Ekenci, Ş. Duyar Özer, R. Capasso, Cruciferous vegetables and their bioactive metabolites: from prevention to novel therapies of colorectal cancer, Evid. Based Complement. Alternat. Med. 2022 (2022), e1534083, https://doi.org/10.1155/2022/1534083.

[20] J. Fernández, B. Silván, R. Entrialgo-Cadierno, C.J. Villar, R. Capasso, J. A. Uranga, F. Lombó, R. Abalo, Antiproliferative and palliative activity of flavonoids in colorectal cancer, Biomed. Pharmacother. 143 (2021), 112241, https://doi.org/10.1016/j.biopha.2021.112241.

[21] F.I. Fahad, N. Barua, M.S. Islam, S.A.J. Sayem, K. Barua, M.J. Uddin, M.N.U. Chy, M. Adnan, M.N. Islam, M.A. Sayeed, T.B. Emran, J. Simal-Gandara, E. Pagano, R. Capasso, Investigation of the pharmacological properties of Lepidagathis hyalina Nees through experimental approaches, Life 11 (2021) 180, https://doi.org/10.3390/life11030180.

[22] S. Hossain, Z. Urbi, H. Karuniawati, R.B. Mohiuddin, A. Moh Qrimida, A.M. M. Allzrag, L.C. Ming, E. Pagano, R. Capasso, Andrographis paniculata (Burm. f.) Wall. ex Nees: an updated review of phytochemistry, antimicrobial pharmacology, and clinical safety and efficacy, Life 11 (2021) 348, https://doi.org/10.3390/life11040348.

[23] M.F. Khan, F.B. Kader, M. Arman, S. Ahmed, C. Lyzu, S.A. Sakib, S.M. Tanzil, A.F. M.I.U. Zim, Md.A.S. Imran, T. Venneri, B. Romano, Md.A. Haque, R. Capasso, Pharmacological insights and prediction of lead bioactive isolates of Dita bark through experimental and computer-aided mechanism, Biomed. Pharmacother. 131 (2020), 110774, https://doi.org/10.1016/j.biopha.2020.110774.

[24] Md.N. Uddin Chy, Md. Adnan, Md.R. Chowdhury, E. Pagano, A.T.M.M. Kamal, K. K. Oh, D.H. Cho, R. Capasso, Central and peripheral pain intervention by Ophiorrhiza rugosa leaves: potential underlying mechanisms and insight into the role of pain modulators, J. Ethnopharmacol. 276 (2021), 114182, https://doi.org/10.1016/j.jep.2021.114182.

[25] M.A. Freitas, A. Vasconcelos, E.C.D. Gonçalves, E.G. Ferrarini, G.B. Vieira, D. Cicia, M. Cola, R. Capasso, R.C. Dutra, Involvement of opioid system and TRPM8/TRPA1 channels in the antinociceptive effect of Spirulina platensis, Biomolecules 11 (2021) 592, https://doi.org/10.3390/biom11040592.

[26] G. Vieira, J. Cavalli, E.C.D. Gonçalves, S.F.P. Braga, R.S. Ferreira, A.R.S. Santos, M. Cola, N.R.B. Raposo, R. Capasso, R.C. Dutra, Antidepressant-like effect of terpineol in an inflammatory model of depression: involvement of the cannabinoid system and D2 dopamine receptor, Biomolecules 10 (2020) 792, https://doi.org/10.3390/biom10050792.

[27] S. Yesmin, A. Paul, T. Naz, A. Rahman, S.F. Akhter, M.I.I. Wahed, T.B. Emran, S. A. Siddiqui, Membrane stabilization as a mechanism of the anti-inflammatory activity of ethanolic root extract of Choi (Piper chaba), Clin. Phytosci. 6 (2020) 1–10, https://doi.org/10.1186/s40816-020-00207-7.

[28] R.N. Chopra, I.C. Chopra, Indigenous Drugs of India, Academic Publishers, 1994.

[29] T. Haque, M.Z. Uddin, Plants used for the beauty care in Dhaka, Bangladesh, Clin. Ex.p Homeopathy 5 (2018) 29–35.
[30] M.E. Haque, A. Rahman, A. Amin, H.U. Shekher, Alkamide and lignan from the stem bark of piper chaba (Piperaceae), Dhaka Univ. J. Pharm. Sci. 3 (2004), https://doi.org/10.3329/dujps.v3i1.187.
[31] I. Chojnowska, K. Kucharczyk, L. Myszkowski, A. Radzikowski, K. Szymańska, Blood serum proteins in experimental chronic liver injury in rabbit, Patol. Pol. 30 (1979) 71–88.
[32] S. Sireeratawong, A. Itharat, N. Lerdvuthisopon, P. Piyabhan, P. Khonsung, S. Boonraeng, K. Jaijoy, Anti-inflammatory, analgesic, and antipyretic activities of the ethanol extract of Piper interruptum Opiz. and Piper chaba Linn, Int. Sch. Res. Not. 2012 (2012), https://doi.org/10.5402/2012/480265.
[33] A. Ghani, Medicinal Plants of Bangladesh: Chemical Constituents and Uses, Asiatic Society of Bangladesh, 1998.
[34] J. Choi, H. Han, The effect of quercetin on the pharmacokinetics of verapamil and its major metabolite, norverapamil, in rabbits, J. Pharm. Pharmacol. 56 (2004) 1537–1542, https://doi.org/10.1211/0022357044814.
[35] M.T. Islam, J. Hasan, H.S.H. Snigdha, E.S. Ali, J. Sharifi-Rad, M. Martorell, M. S. Mubarak, Chemical profile, traditional uses, and biological activities of Piper chaba Hunter: a review, J. Ethnopharmacol. 257 (2020), 112853, https://doi.org/10.1016/j.jep.2020.112853.
[36] H. Matsuda, K. Ninomiya, T. Morikawa, D. Yasuda, I. Yamaguchi, M. Yoshikawa, Hepatoprotective amide constituents from the fruit of Piper chaba: structural requirements, mode of action, and new amides, Bioorg. Med. Chem. 17 (2009) 7313–7323, https://doi.org/10.1016/j.bmc.2009.08.050.
[37] M. Hossain, M. Mondal, R.U. Morad, N. Uddin, A. Das, M.M. Kamal, M. Islam, T. B. Wahed, M.M.H. Chowdhury, Evaluation of bioactivities of methanol and petroleum ether extracts of Cassia renigera seed, Clin. Phytosci. 4 (2018) 1–10, https://doi.org/10.1186/s40816-018-0091-x.
[38] I. Asif, M. Mahmood, M. Alam, M. Khan, S. Eti, F. Hossain, M. Moniruzzaman, M. Islam, Studies on Coriandrum sativum Linn seed of different origin of Bangladesh for its essential oil, fatty oil and micronutrients, BangladeshJ. Sci. Ind. Res. 48 (2013) 221–228, https://doi.org/10.3329/bjsir.v48i4.18272.
[39] T.B. Wahed, M. Mondal, M.A. Rahman, M.S. Hossen, N.C. Bhoumik, S. Saha, E. Tanvir, M.I. Khalil, S.K. Kundu, M.T. Islam, Protective role of Syzygium Cymosum leaf extract against carbofuran-induced hematological and hepatic toxicities, Chem. Res. Toxicol. 32 (2019) 1619–1629, https://doi.org/10.1021/acs.chemrestox.9b00164.
[40] M. Mondal, S. Saha, M. Hossain, I. Al Foyjul, C. Sarkar, S. Hossain, A.B. R. Khalipha, S.K. Kundu, Phytochemical profiling and evaluation of bioactivities of methanolic and ethyl acetate extracts of Marsdenia tenacissima leaves, Int. J. Geogr. Inf. Syst. 26 (2020) 405–422, https://doi.org/10.1080/10496475.2020.1748784.
[41] M. Mondal, M. Hossain, N. Das, M.A. Rahman, N. Uddin, M. Hasan, M. Alam, M. Islam, T.B. Wahed, S.K. Kundu, Investigation of bioactivities of methanolic and ethyl acetate extracts of Dioscorea pentaphylla leaf along with its phenolic composition, J. Food Meas. Charact. 13 (2019) 622–633, https://doi.org/10.1007/s11694-018-9975-1.
[42] A. Rajasekaran, M. Periyasamy, Hepatoprotective effect of ethanolic extract of Trichosanthes lobata on paracetamol-induced liver toxicity in rats, Chin. Med. 7 (2012) 1–6, https://doi.org/10.1186/1749-8546-7-12.
[43] M. Mondal, C. Sarkar, S. Saha, M.N. Hossain, R. Norouzi, M.S. Mubarak, A. Siyadatpanah, P. Wilairatana, R. Hossain, M.T. Islam, Hepatoprotective activity of andrographolide possibly through antioxidative defense mechanism in Sprague-Dawley rats, Toxicol. Rep. 9 (2022) 1013–1022, https://doi.org/10.1016/j.toxrep.2022.04.007.
[44] M. Mondal, M.M. Hossain, M.A. Rahman, S. Saha, N. Uddin, M.R. Hasan, A. Kader, T.B. Wahed, S.K. Kundu, M.T. Islam, Hepatoprotective and antioxidant activities of Justicia gendarussa leaf extract in carbofuran-induced hepatic damage in rats, Chem. Res. Toxicol. 32 (2019) 2499–2508, https://doi.org/10.1021/acs.chemrestox.9b00345.
[45] M. Mondal, M.M. Hossain, M.R. Hasan, M.T.I. Tarun, M.A.F. Islam, M. Choudhuri, M.T. Islam, M.S. Mubarak, Hepatoprotective and antioxidant capacity of Mallotus repandus ethyl acetate stem extract against D-galactosamine-induced hepatotoxicity in rats, ACS Omega 5 (2020) 6523–6531, https://doi.org/10.1021/acsomega.9b04189.
[46] M. Mondal, M.S. Hossen, M.A. Rahman, S. Saha, C. Sarkar, N.C. Bhoumik, S. K. Kundu, Antioxidant mediated protective effect of Bridelia tomentosa leaf extract against carbofuran induced oxidative hepatic toxicity, Toxicol. Rep. 8 (2021) 1369–1380, https://doi.org/10.1016/j.toxrep.2021.07.003.
[47] M. Mondal, S.K. Kundu, M.T. Islam, Ž. Reiner, M. Martorell, J. Sharifi-Rad, Protective effect of Bridelia tomentosa due to its phenolic acids and flavonoids against oxidative stress-mediated hepatic toxicity induced by carbofuran, S.Afr. J. Bot. 141 (2021) 447–456, https://doi.org/10.1016/j.sajb.2021.06.006.
[48] M.T. Islam, C. Quispe, M.A. Islam, E.S. Ali, S. Saha, U.H. Asha, M. Mondal, A.F. A. Razis, U. Sunusi, R.M. Kamal, Effects of nerol on paracetamol-induced liver damage in Wistar albino rats, Biomed. Pharmacother. 140 (2021), 111732, https://doi.org/10.1016/j.biopha.2021.111732.
[49] M. Mondal, S. Saha, C. Sarkar, M.S. Hossen, M.S. Hossain, A.B.R. Khalipha, M. F. Islam, T.B. Wahed, M.T. Islam, A. Rauf, Role of Citrus medica L. fruits extract in combatting the hematological and hepatic toxic effects of carbofuran, Chem. Res. Toxicol. 34 (2021) 1890–1902, https://doi.org/10.1021/acs.chemrestox.1c00166.
[50] C. Chen, X. Liu, S. Qi, A.C. Dias, J. Yan, X. Zhang, Hepatoprotective effect of Phellinus linteus mycelia polysaccharide (PL-N1) against acetaminophen-induced liver injury in mouse, Int. J. Biol. Macromol. 154 (2020) 1276–1284, https://doi.org/10.1016/j.ijbiomac.2019.11.002.
[51] C. Sarkar, S. Jamaddar, M. Mondal, A.B.R. Khalipha, M.T. Islam, M.S. Mubarak, Natural products as anti-COVID-19 agents: an in silico study, Coronaviruses 2 (2020) 10–17, https://doi.org/10.2174/2666796701999201116124851.
[52] M. Mondal, C. Sarkar, S. Jamaddar, A.B. Khalipha, M.T. Islam, A. Mahafzah, M. S. Mubarak, Evaluation of the binding affinity of anti-viral drugs against main protease of SARS-CoV-2 through a molecular docking study, Infect. Disord.-Drug Targets 21 (2021) 37–43, https://doi.org/10.2174/1871526520666201207124408.
[53] M. Mondal, C. Quispe, C. Sarkar, T.C. Bepari, M.J. Alam, S. Saha, P. Ray, M. A. Rahim, M.T. Islam, W.N. Setzer, Analgesic and anti-inflammatory potential of essential oil of Eucalyptus camaldulensis leaf:in vivo and in silico studies, Nat. Prod. Commun. 16 (2021), https://doi.org/10.1177/1934578X211007634, 1934578X211007634.
[54] C. Sarkar, M. Abdalla, M. Mondal, A.B.R. Khalipha, N. Ali, Ebselen suitably interacts with the potential SARS-CoV-2 targets: an in-silico approach, J. Biomol. Struct. Dyn. (2021) 1–16, https://doi.org/10.1080/07391102.2021.1971562.
[55] N. Kumar, S. Gupta, T. Chand Yadav, V. Pruthi, P. Kumar Varadwaj, N. Goel, Extrapolation of phenolic compounds as multi-target agents against cancer and inflammation, J. Biomol. Struct. Dyn. 37 (2019) 2355–2369, https://doi.org/10.1080/07391102.2018.1481457.
[56] M.O. Rafi, K. Al-Khafaji, T.T. Tok, M.S. Rahman, Computer-based identification of potential compounds from Salviae miltiorrhizae against Neirisaral adhesion A regulatory protein, J. Biomol. Struct. Dyn. (2020) 1–13, https://doi.org/10.1080/07391102.2020.1856189.
[57] R. Shukla, N.S. Munjal, T.R. Singh, Identification of novel small molecules against GSK3β for Alzheimer's disease using chemoinformatics approach, J. Mol. Graph. Model. 91 (2019) 91–104, https://doi.org/10.1016/j.jmgm.2019.06.008.
[58] M.J. Abraham, T. Murtola, R. Schulz, S. Páll, J.C. Smith, B. Hess, E. Lindahl, GROMACS: high performance molecular simulations through multi-level parallelism from laptops to supercomputers, SoftwareX 1 (2015) 19–25, https://doi.org/10.1016/j.softx.2015.06.001.
[59] P. Bjelkmar, P. Larsson, M.A. Cuendet, B. Hess, E. Lindahl, Implementation of the CHARMM force field in GROMACS: analysis of protein stability effects from correction maps, virtual interaction sites, and water models, J. Chem. Theory Comput. 6 (2010) 459–466, https://doi.org/10.1021/ct900549r.
[60] V. Zoete, M.A. Cuendet, A. Grosdidier, O. Michielin, SwissParam: a fast force field generation tool for small organic molecules, J. Comput. Chem. 32 (2011) 2359–2368, https://doi.org/10.1002/jcc.21816.
[61] K. Al-Khafaji, T. Taskin Tok, Amygdalin as multi-target anticancer drug against targets of cell division cycle: double docking and molecular dynamics simulation, J. Biomol. Struct. Dyn. 39 (2021) 1965–1974, https://doi.org/10.1080/07391102.2020.1742792.
[62] Md.O. Rafi, G. Bhattacharje, K. Al-Khafaji, T. Taskin-Tok, Md.A. Alfasane, A. K. Das, Md.A.K. Parvez, Md.S. Rahman, Combination of QSAR, molecular docking, molecular dynamic simulation and MM-PBSA: analogues of lopinavir and favipiravir as potential drug candidates against COVID-19, J. Biomol. Struct. Dyn. 40 (2022) 3711–3730, https://doi.org/10.1080/07391102.2020.1850355.
[63] T. Darden, D. York, L. Pedersen, Particle mesh Ewald: an N· log (N) method for Ewald sums in large systems, J. Chem. Phys. 98 (1993) 10089–10092, https://doi.org/10.1063/1.464397.
[64] Z. Chauhdary, U. Dr, B. Saleem, S. Ahmad, M.A.Sh.ah. Shah, Neuroprotective evaluation of Tribulus terrestris L. in aluminum chloride induced Alzheimer's disease, Pak. J. Pharm. Sci. 32 (2019) 805–816.
[65] S.S. Lee, J.T. Buters, T. Pineau, P. Fernandez-Salguero, F.J. Gonzalez, Role of CYP2E1 in the hepatotoxicity of acetaminophen (*), J. Biol. Chem. 271 (1996) 12063–12067, https://doi.org/10.1074/jbc.271.20.12063.
[66] S.S. Kalsi, D.M. Wood, W.S. Waring, P.I. Dargan, Does cytochrome P450 liver isoenzyme induction increase the risk of liver toxicity after paracetamol overdose? Open Access Emerg. Med. 3 (2011) 69, https://doi.org/10.2147/OAEM.S24962.
[67] M. Yayla, Z. Halici, B. Unal, Y. Bayir, E. Akpinar, F. Gocer, Protective effect of Et-1 receptor antagonist bosentan on paracetamol induced acute liver toxicity in rats, Eur. J. Pharmacol. 726 (2014) 87–95, https://doi.org/10.1016/j.ejphar.2014.01.022.
[68] J.E. Okokon, P.A. Nwafor, U. Charles, A. Dar, M. Iqbal Choudhary, Antioxidative burst and hepatoprotective effects of ethanol root extract of Hippocratea africana against paracetamol-induced liver injury, Pharm. Biol. 51 (2013) 872–880, https://doi.org/10.3109/13880209.2013.768273.
[69] E. Sinaga, A. Fitrayadi, A. Asrori, S.E. Rahayu, S. Suprihatin, V.D. Prasasty, Hepatoprotective effect of Pandanus odoratissimus seed extracts on paracetamol-induced rats, Pharm. Biol. 59 (2021) 31–39, https://doi.org/10.1080/13880209.2020.1865408.
[70] C. Delgado-Montemayor, P. Cordero-Pérez, R. Salazar-Aranda, N. Waksman-Minsky, Models of hepatoprotective activity assessment, Med. Univ. 17 (2015) 222–228, https://doi.org/10.1016/j.rmu.2015.10.002.
[71] M.K. Rasool, E.P. Sabina, S.R. Ramya, P. Preety, S. Patel, N. Mandal, P.P. Mishra, J. Samuel, Hepatoprotective and antioxidant effects of gallic acid in paracetamol-induced liver damage in mice, J. Pharm. Pharmacol. 62 (2010) 638–643, https://doi.org/10.1211/jpp.62.05.0012.
[72] N.S. Uchida, S.E. Silva-Filho, G.F.E. Cardia, E. Cremer, F.M.de S. Silva-Comar, E. L. Silva, C.A. Bersani-Amado, R.K.N. Cuman, Hepatoprotective effect of citral on acetaminophen-induced liver toxicity in mice, Evid. Based Complement. Alternat. Med. 2017 (2017), https://doi.org/10.1155/2017/1796209.

[73] J.H. Donfack, G.W. Fotso, B. Ngameni, F.N. Tsofack, A. Tchoukoua, P. Ambassa, W. Abia, A. Tchana, S. Giardina, D. Buonocore, In vitro hepatoprotective and antioxidant activities of the crude extract and isolated compounds from Irvingia gabonensis, 亚洲传统医药 5 (2010) 79–88.
[74] J.E. Okokon, J.O. Simeon, E.E. Umoh, Hepatoprotective activity of the extract of Homalium letestui stem against paracetamol-induced liver injury, Avicenna J. Phytomedicine 7 (2017) 27.
[75] O.L. Aberare, P. Okuonghae, N. Mukoro, J.O. Dirisu, F. Osazuwa, E. Odigie, R. Omoregie, Triglycerides, total cholesterol, high density lipoprotein cholesterol and low density lipoprotein cholesterol in rats exposed to premium motor spirit fumes, North Am. J. Med. Sci. 3 (2011) 277, https://doi.org/10.4297/najms.2011.3277.
[76] H.R.B. Raghavendran, A. Sathivel, T. Devaki, Effect of Sargassum polycystum (Phaeophyceae)-sulphated polysaccharide extract against acetaminophen-induced hyperlipidemia during toxic hepatitis in experimental rats, Mol. Cell. Biochem. 276 (2005) 89–96, https://doi.org/10.1007/s11010-005-3194-x.
[77] M.A. Shah, H. Muhammad, Y. Mehmood, R. Khalil, Z. Ul-Haq, P. Panichayupakaranant, Superoxide scavenging and antiglycation activity of Rhinacanthins-rich extract obtained from the leaves of Rhinacanthus nasutus, Pharmacogn. Mag. 13 (2017) 652–658, https://doi.org/10.4103/pm.pm_196_17.
[78] A. Grypioti, G. Kostopanagiotou, M. Mykoniatis, Platelet-activating factor inactivator (rPAF-AH) enhances liver's recovery after paracetamol intoxication, Dig. Dis. Sci. 52 (2007) 2580–2590, https://doi.org/10.1007/s10620-006-9728-6.
[79] L. Yuan, N. Kaplowitz, Glutathione in liver diseases and hepatotoxicity, Mol. Asp. Med. 30 (2009) 29–41, https://doi.org/10.1016/j.mam.2008.08.003.
[80] R. Standish, E. Cholongitas, A. Dhillon, A. Burroughs, A. Dhillon, An appraisal of the histopathological assessment of liver fibrosis, Gut 55 (2006) 569–578, https://doi.org/10.1136/gut.2005.084475.
[81] N. Mahmood, S. Mamat, F. Kamisan, F. Yahya, M. Kamarolzaman, N. Nasir, N. Mohtarrudin, S. Tohid, Z. Zakaria, Amelioration of paracetamol-induced hepatotoxicity in rat by the administration of methanol extract of Muntingia calabura L. leaves, Biomed. Res. Int. 2014 (2014), https://doi.org/10.1155/2014/695678.
[82] G.C.L. Ee, C.M. Lim, C.K. Lim, M. Rahmani, K. Shaari, C.F.J. Bong, Alkaloids from Piper sarmentosum and Piper nigrum, Nat. Prod. Res. 23 (2009) 1416–1423, https://doi.org/10.1080/14786410902757998.
[83] S. Islam, A.C. Roy, M. Haque, S. Hossain, M. Abu, PHYTOCHEMICAL STUDIES ON PIPER CHABA HUNTER, Int. J. Pharm. Sci. Res. 6 (n.d.) 8.
[84] E.P. Sabina, A.D.H. Souriyan, D. Jackline, M.K. Rasool, Piperine, an active ingredient of black pepper attenuates acetaminophen–induced hepatotoxicity in mice, Asian Pac.J. Trop. Med. 3 (2010) 971–976, https://doi.org/10.1016/S1995-7645(11)60011-4.
[85] I. Koul, A. Kapil, Evaluation of the liver protective potential of piperine, an active principle of black and long peppers, Planta Med. 59 (1993) 413–417, https://doi.org/10.1055/s-2006-959721.
[86] M.A. Morsy, N.S. Younis, A.A.K. El-Sheikh, F.H.Al Turaifi, M. El-Daly, O. M. Mohafez, Protective mechanisms of piperine against acetaminophen-induced hepatotoxicity may be mediated through TGFBRAP1, Eur. Rev. Med. Pharmacol. Sci. 24 (2020) 10169–10180, https://doi.org/10.26355/eurrev_202010_23237.
[87] S.K. Desai, V.S. Gawali, A.B. Naik, L.L. D'souza, Potentiating effect of piperine on hepatoprotective activity of Boerhaavia diffusa to combat oxidative stress, Int. J. Pharmacol. 4 (2008) 393–397, https://doi.org/10.3923/ijp.2008.393.397.
[88] D. Rathee, A. Kamboj, R.K. Sachdev, S. Sidhu, Hepatoprotective effect of Aegle marmelos augmented with piperine co-administration in paracetamol model, Rev. Bras. Farmacogn. 28 (2018) 65–72, https://doi.org/10.1016/j.bjp.2017.11.003.
[89] P. Rinwa, A. Kumar, Piperine potentiates the protective effects of curcumin against chronic unpredictable stress-induced cognitive impairment and oxidative damage in mice, Brain Res. 1488 (2012) 38–50, https://doi.org/10.1016/j.brainres.2012.10.002.
[90] O.A. Adeyemo, A. Ore, E.O. Ajisafe, The protective effect of piperine on oxidative stress and hepatic damage induced by diisononyl phthalate in rat, Egypt. J. Basic Appl. Sci. 8 (2021) 293–301, https://doi.org/10.1080/2314808X.2021.1983746.
[91] A.M. Abdelhamid, A. Selim, M.A. Zaafan, The hepatoprotective effect of piperine against thioacetamide-induced liver fibrosis in mice: the involvement of miR-17 and TGF-β/Smads pathways, Front. Mol. Biosci. 8 (2021), 754098, https://doi.org/10.3389/fmolb.2021.754098.
[92] M.T. Islam, E.S. Ali, S.J. Uddin, S. Shaw, M.A. Islam, M.I. Ahmed, M. Chandra Shill, U.K. Karmakar, N.S. Yarla, I.N. Khan, M.M. Billah, M. D. Pieczynska, G. Zengin, C. Malainer, F. Nicoletti, D. Gulei, I. Berindan-Neagoe, A. Apostolov, M. Banach, A.W.K. Yeung, A. El-Demerdash, J. Xiao, P. Dey, S. Yele, A. Jóźwik, N. Strzałkowska, J. Marchewka, K.R.R. Rengasamy, J. Horbańczuk, M. A. Kamal, M.S. Mubarak, S.K. Mishra, J.A. Shilpi, A.G. Atanasov, Phytol: a review of biomedical activities, Food Chem. Toxicol. 121 (2018) 82–94, https://doi.org/10.1016/j.fct.2018.08.032.
[93] K. Gupta, T. Taj, B. Thansiya, J.V. Kamath, Pre-clinical evaluation of hepatoprotective activity of phytol in wistar albino rats, IP Int. J. Compr. Adv. Pharmacol. 4 (2019) 17–20, https://doi.org/10.18231/j.ijcaap.2019.004.
[94] S.H. Jeong, Inhibitory effect of phytol on cellular senescence, Biomed. Dermatol. 2 (2018) 13, https://doi.org/10.1186/s41702-018-0025-8.
[95] E.A. Abd El-Ghffar, H.A.S. El-Nashar, O.A. Eldahshan, A.N.B. Singab, GC-MS analysis and hepatoprotective activity of the n-hexane extract of Acrocarpus fraxinifolius leaves against paracetamol-induced hepatotoxicity in male albino rats, Pharm. Biol. 55 (2017) 441–449, https://doi.org/10.1080/13880209.2016.1246575.
[96] M.S. Salvadori, V.G. Mota, L.M. Costa, A.A.C. de Almeida, G.A.L. de Oliveira, J. P. Costa, D.P. de Sousa, R.M. de Freitas, R.N. de Almeida, Antinociceptive and antioxidant activities of phytol in vivo and in vitro models, Neurosci. J. 2013 (2013) 1–9, https://doi.org/10.1155/2013/949452.
[97] R. Srinivasan, K.R. Devi, A. Kannappan, S.K. Pandian, A.V. Ravi, Piper betle and its bioactive metabolite phytol mitigates quorum sensing mediated virulence factors and biofilm of nosocomial pathogen Serratia marcescens in vitro, J. Ethnopharmacol. 193 (2016) 592–603, https://doi.org/10.1016/j.jep.2016.10.017.
[98] G.C.L. Ee, C.M. Lim, M. Rahmani, K. Shaari, C.F.J. Bong, Pellitorine, a potential anti-cancer lead compound against HL60 and MCT-7 cell lines and microbial transformation of piperine from Piper nigrum, Molecules 15 (2010) 2398–2404, https://doi.org/10.3390/molecules15042398.
[99] A. Usmani, M. Mujahid, M. Khushtar, H.H. Siddiqui, M.A. Rahman, Hepatoprotective effect of Anacyclus pyrethrum Linn. against antitubercular drug-induced hepatotoxicity in SD rats, J. Complement. Integr. Med. 13 (2016) 295–300, https://doi.org/10.1515/jcim-2016-0001.
[100] Identification of chemical constituents of Zanthoxylum heitzii stem bark and their insecticidal activity against the malaria mosquito Anopheles gambiae | Parasites & Vectors | Full Text, (n.d.). https://parasitesandvectors.biomedcentral.com/articles/10.1186/s13071-015-1113-x (accessed June 16, 2022).
[101] W. Lee, S.-K. Ku, B.-W. Min, S. Lee, J.-G. Jee, J.A. Kim, J.-S. Bae, Vascular barrier protective effects of pellitorine in LPS-induced inflammation in vitro and in vivo, Fitoterapia 92 (2014) 177–187, https://doi.org/10.1016/j.fitote.2013.11.006.
[102] P. Anandakumar, S. Kamaraj, M.K. Vanitha, D-limonene: a multifunctional compound with potent therapeutic effects, J. Food Biochem. 45 (2021), https://doi.org/10.1111/jfbc.13566.
[103] D. IndumathiSelvanathan, D.S. Arumugham, S.M.F.M. Begum, Hepatoprotective effect of d-limonene against adriamycin induced hepatotoxicity in experimental rats, Eur. J. Mol. Clin. Med. 7 (2021) 7712–7721.
[104] R. Amini, M. Asle-Rousta, S. Aghazadeh, Hepatoprotective effect of limonene against chronic immobilization induced liver damage in rats, Naunyn. SchmiedebergsArch. Pharmacol. 393 (2020) 2053–2059, https://doi.org/10.1007/s00210-020-01915-0.
[105] R.M. AlSaffar, S. Rashid, S.B. Ahmad, M.U. Rehman, I. Hussain, S. Parvaiz Ahmad, M.A. Ganaie, D-limonene (5 (one-methyl-four-[1-methylethenyl]) cyclohexane) diminishes CCl4-induced cardiac toxicity by alleviating oxidative stress, inflammatory and cardiac markers, Redox Rep. 27 (2022) 92–99, https://doi.org/10.1080/13510002.2022.2062947.
[106] Y. Tambe, H. Tsujiuchi, G. Honda, Y. Ikeshiro, S. Tanaka, Gastric cytoprotection of the non-steroidal anti-inflammatory sesquiterpene, β-caryophyllene, Planta Med. 62 (1996) 469–470, https://doi.org/10.1055/s-2006-957942.
[107] M.E. Kelany, M.A. Abdallah, Protective effects of combined β-caryophyllene and silymarin against ketoprofen-induced hepatotoxicity in rats, Can. J. Physiol. Pharmacol. 94 (2016) 739–744, https://doi.org/10.1139/cjpp-2015-0607.
[108] M.A. Calleja, J.M. Vieites, T. Montero-Meterdez, M.I. Torres, M.J. Faus, A. Gil, A. Suárez, The antioxidant effect of β-caryophyllene protects rat liver from carbon tetrachloride-induced fibrosis by inhibiting hepatic stellate cell activation, Br. J. Nutr. 109 (2013) 394–401, https://doi.org/10.1017/S0007114512001298.
[109] B. Dwivedi, S. Kumar, C. Nayak, B. Mehta, Gas chromatography mass spectrometry (GC-MS) analysis of the hexane and benzene extracts of the Piper betle (leaf stalk) (Family: Piperaceae) from India, J. Med. Plants Res. 4 (2010).
[110] M.E.A. Pinto, S.G. Araújo, M.I. Morais, N.P. Sá, C.M. Lima, C.A. Rosa, E. P. Siqueira, S. Johann, L.a.R.S. Lima, Antifungal and antioxidant activity of fatty acid methyl esters from vegetable oils, An. Acad. Bras. Ciênc. 89 (2017) 1671–1681, https://doi.org/10.1590/0001-3765201720160908.
[111] M.T. Shaaban, M.F. Ghaly, S.M. Fahmi, Antibacterial activities of hexadecanoic acid methyl ester and green-synthesized silver nanoparticles against multidrug-resistant bacteria, J. Basic Microbiol. 61 (2021) 557–568, https://doi.org/10.1002/jobm.202100061.
[112] M. Gupta, A. Gupta, S. Gupta, In vitro antimicrobial and phytochemical analysis of dichloromethane extracts of Piper nigrum (black pepper), Orient. J. Chem. 29 (2013) 777–782, https://doi.org/10.13005/ojc/290259.
[113] P.Kumar Bellamakondi, A. Godavarthi, M. Ibrahim, Caralluma umbellata Haw. protects liver against paracetamol toxicity and inhibits CYP2E1, BioImpacts BI 8 (2018) 23–30, https://doi.org/10.15171/bi.2018.04.
[114] P. Hasanein, M. Sharifi, Effects of rosmarinic acid on acetaminophen-induced hepatotoxicity in male Wistar rats, Pharm. Biol. 55 (2017) 1809–1816, https://doi.org/10.1080/13880209.2017.1331248.
[115] A. Khelfallah, B. Aouay, M. Kebieche, H. Fetoui, CYP2E1 inhibition and NF_κB signaling pathway are involved in the protective molecular effect of Origanum floribundum against acetaminophen-induced acute hepatotoxicity in rats, Iran. J. Pharm. Res. 20 (2021) 577–591, https://doi.org/10.22037/ijpr.2021.114487.14878.
[116] J.-W. Ko, J.-Y. Shin, J.-W. Kim, S.-H. Park, N.-R. Shin, I.-C. Lee, I.-S. Shin, C. Moon, S.-H. Kim, S.-H. Kim, J.-C. Kim, Protective effects of diallyl disulfide against acetaminophen-induced nephrotoxicity: a possible role of CYP2E1 and NF-κB, Food Chem. Toxicol. 102 (2017) 156–165, https://doi.org/10.1016/j.fct.2017.02.021.
[117] R. Hossain, K. Al-Khafaji, R.A. Khan, C. Sarkar, M.S. Islam, D. Dey, D. Jain, F. Faria, R. Akbor, O. Atolani, S.M.R. Oliveira, A. Siyadatpanah, M.de L. Pereira, M.T. Islam, Quercetin and/or ascorbic acid modulatory effect on phenobarbital-

induced sleeping mice possibly through GABAA and GABAB receptor interaction pathway, Pharmaceuticals 14 (2021) 721, https://doi.org/10.3390/ph14080721.
[118] S. Beckmann-Knopp, S. Rietbrock, R. Weyhenmeyer, R.H. Böcker, K.T. Beckurts, W. Lang, M. Hunz, U. Fuhr, Inhibitory effects of silibinin on cytochrome P-450 enzymes in human liver microsomes, Pharmacol. Toxicol. 86 (2000) 250–256, https://doi.org/10.1111/j.0901-9928.2000.860602.x.
[119] K.M. Comar, D.F. Kirby, Herbal remedies in gastroenterology, J. Clin. Gastroenterol. 39 (2005) 457–468, https://doi.org/10.1097/01.mcg.0000165650.09500.3a.